

Living at the edge of stability: The role of continuum and three-nucleon forces.

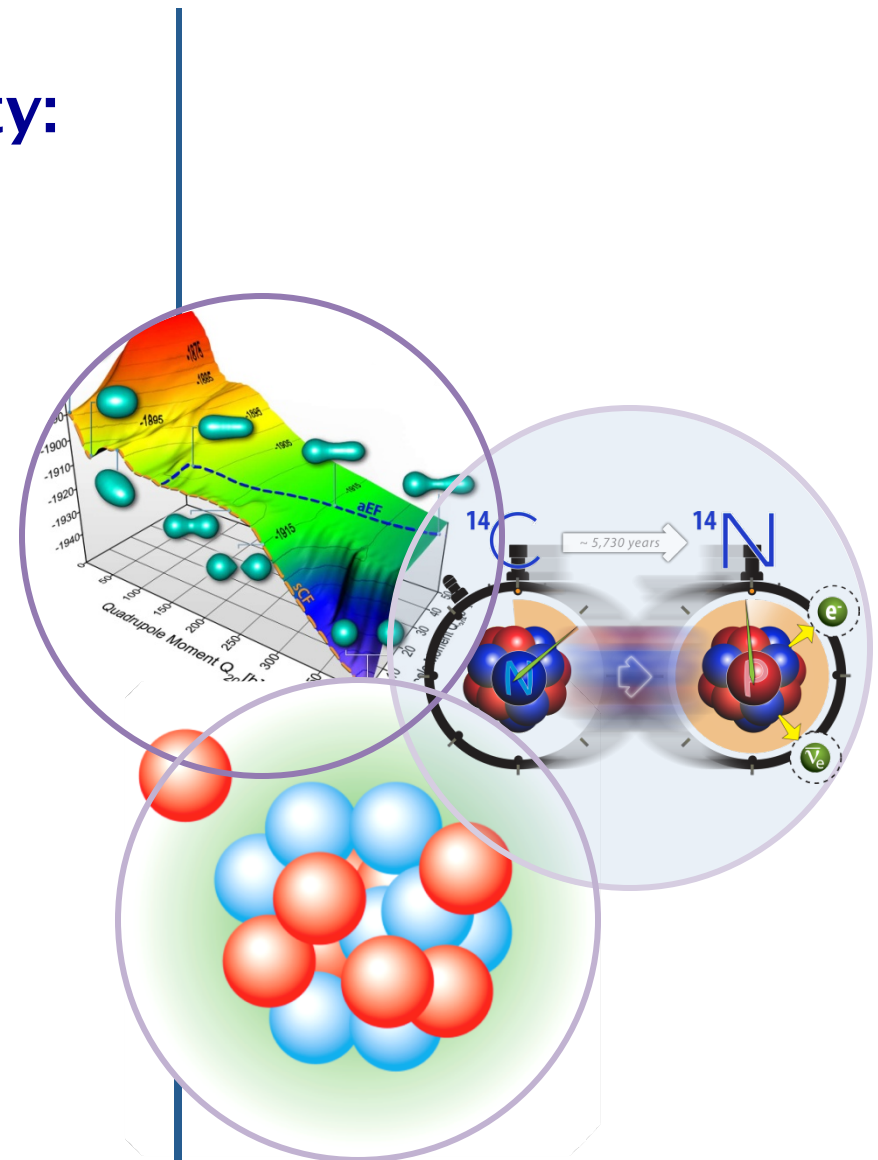
Gaute Hagen (ORNL)

Collaborators:

Morten Hjorth-Jensen (UiO/CMA)
Gustav Jansen (UiO/CMA)
Ruprecht Machleidt (UI)
Nicolas Michel (UT)
Thomas Papenbrock (UT/ORNL)

Light Nuclei from first principles: Structure of light nuclei

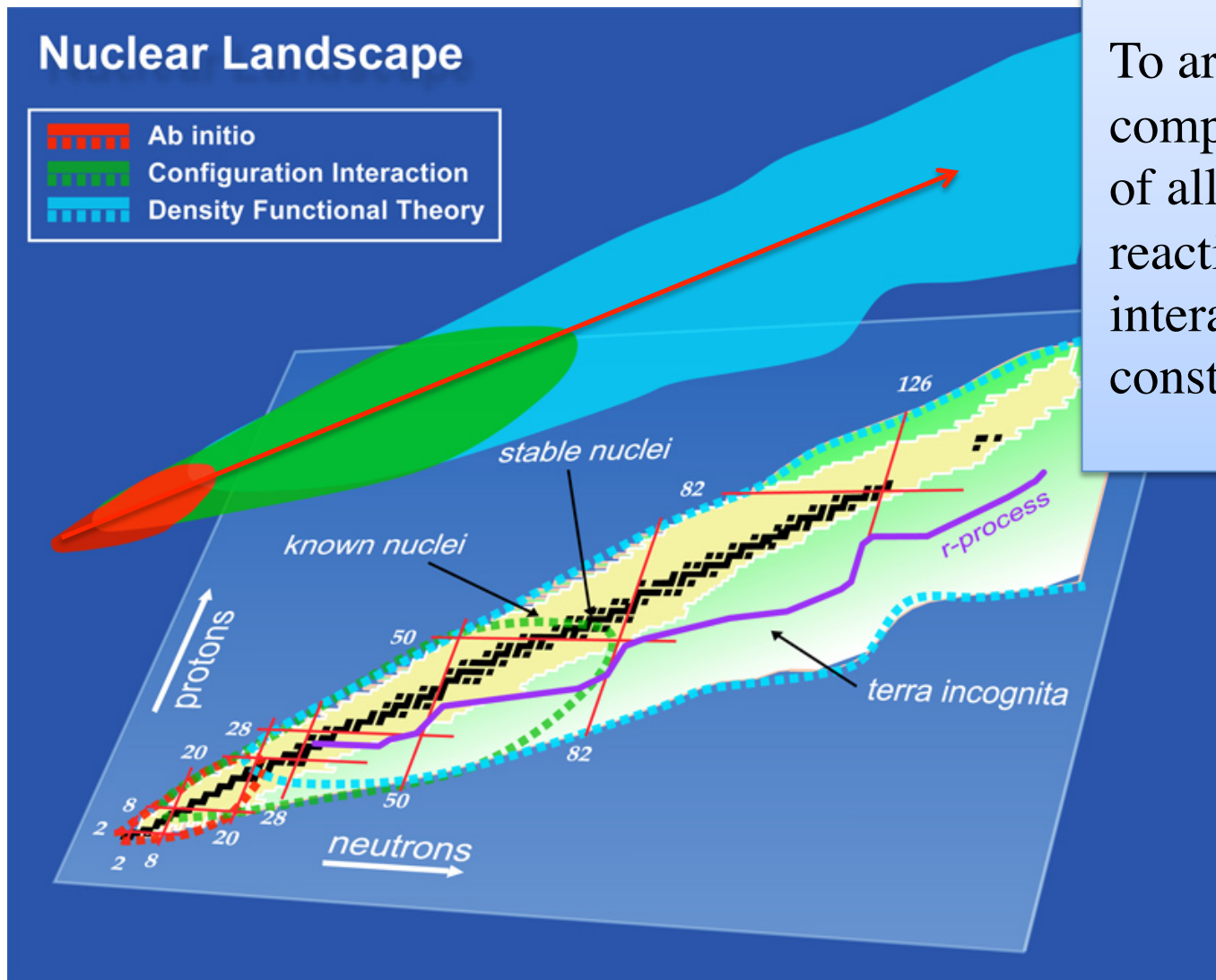
INT, October 10, 2012



Outline

1. Interactions from chiral EFT and Coupled-Cluster theory
2. Open-quantum systems: how to describe physics of nuclei at the edge of stability?
3. Role of continuum and three-nucleon forces in neutron rich oxygen isotopes
4. Evolution of shell structure in neutron rich calcium isotopes
5. Elastic proton scattering of medium mass nuclei from coupled-cluster theory
6. Densities of neutron rich oxygen isotopes – Resolving the anomalous cross section of ^{23}O

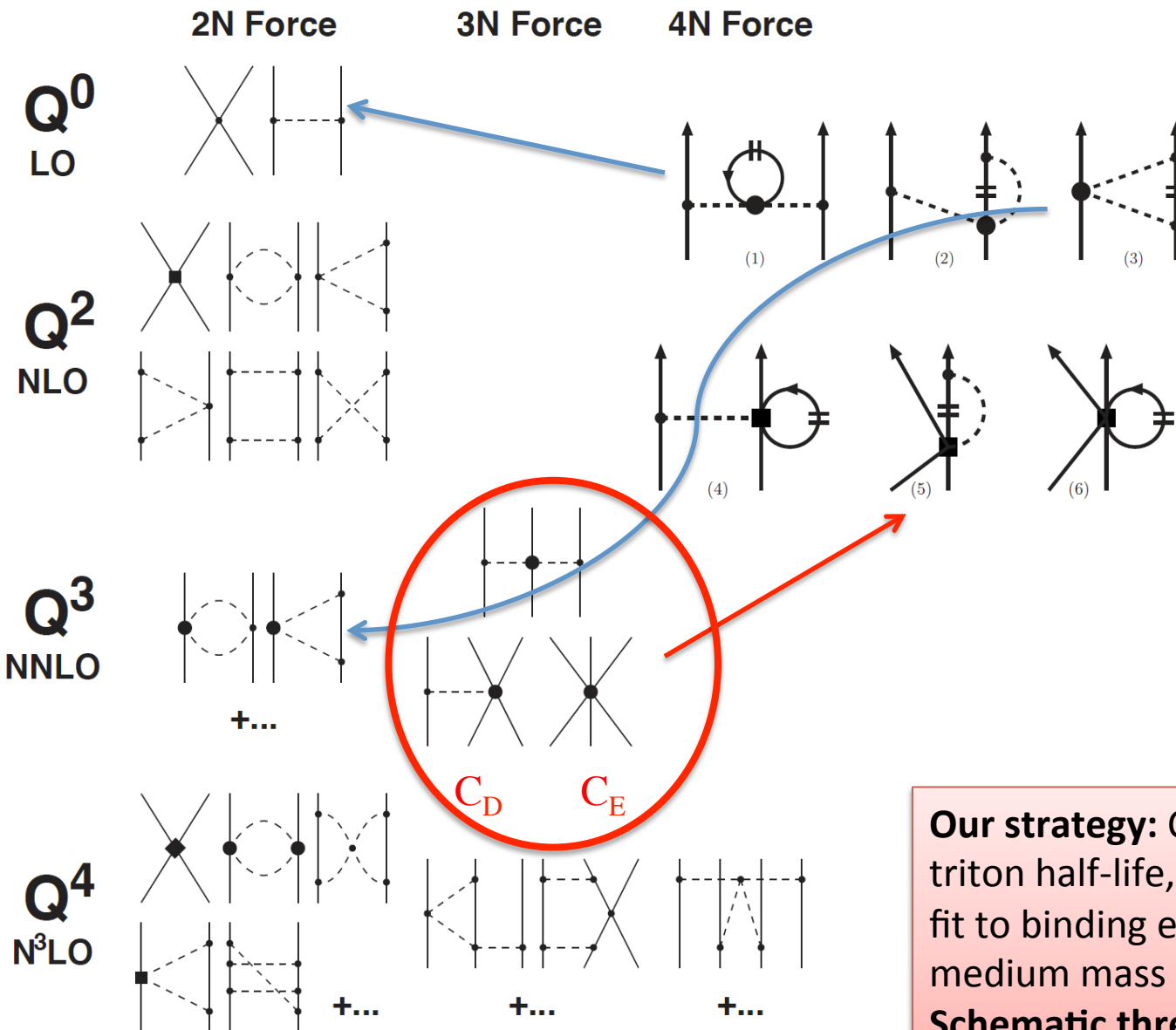
Roadmap for Theory of Nuclei



Main goal :

To arrive at a comprehensive description of all nuclei and low-energy reactions from the basic interactions between the constituent nucleons

Three-nucleon forces as in-medium corrections to nucleon-nucleon forces

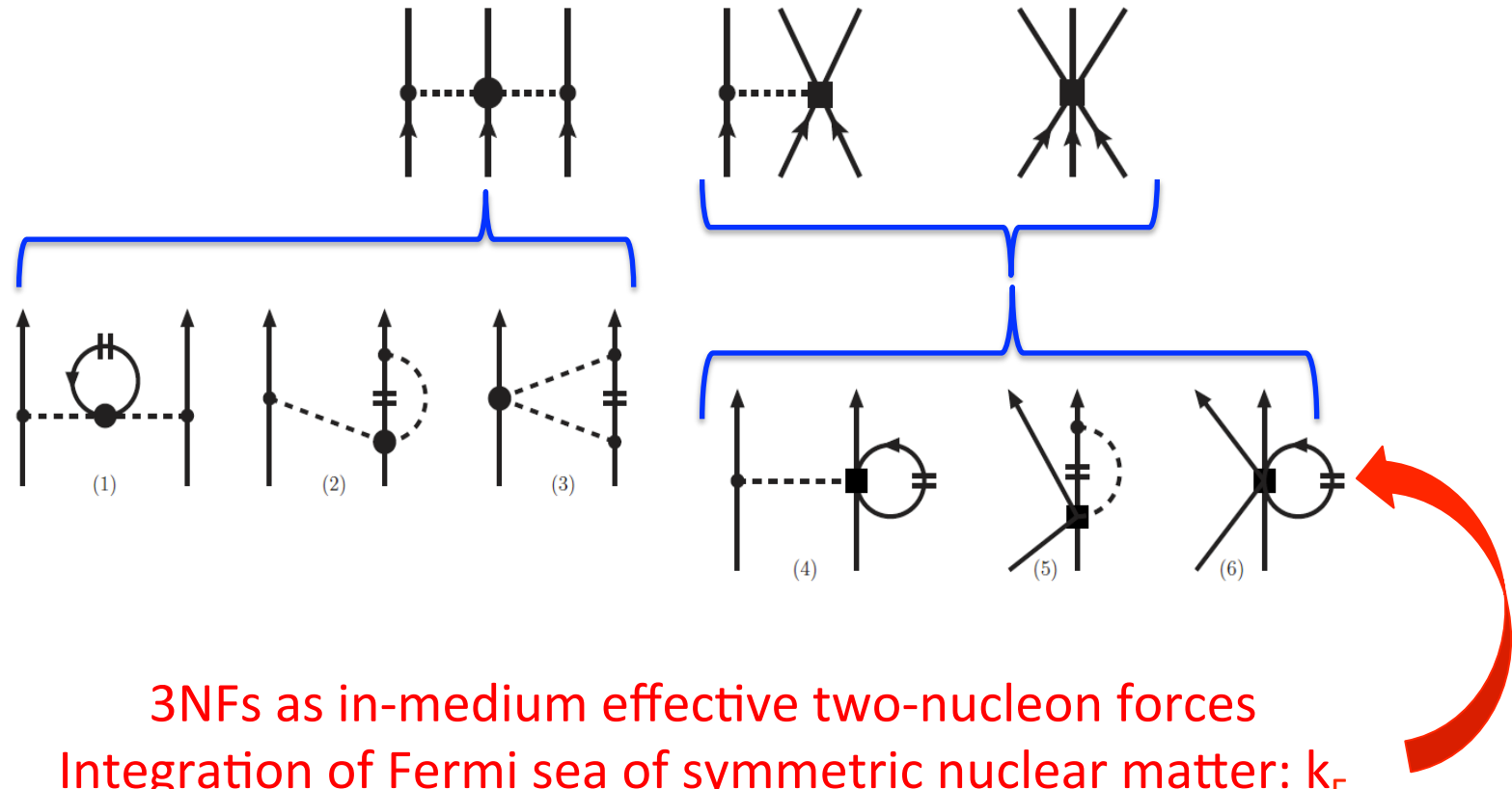


Integrating over the third leg in infinite nuclear matter and derive density dependent corrections to the nucleon-nucleon interaction.
 J. W. Holt N. Kaiser and W. Weise. Phys.Rev.C 79, 054331 (2009)
 K. Hebeler and A. Schwenk (2010)

Our strategy: C_D is given by fit to triton half-life, we fix C_E and k_F from fit to binding energy in selected medium mass nuclei:
Schematic three-nucleon forces

Including the effects of 3NFs (approximation!)

[J.W. Holt, Kaiser, Weise, PRC 79, 054331 (2009); Hebeler & Schwenk, PRC 82, 014314 (2010)]



Parameters: For Oxygen we use $k_F = 1.05 \text{ fm}^{-1}$, $c_E = 0.71$, $c_D = -0.2$ from binding energies of $^{16,22}\text{O}$, for Calcium we use $k_F = 0.95 \text{ fm}^{-1}$, $c_E = 0.735$, $c_D = -0.2$ from binding energy of ^{48}Ca and ^{52}Ca (The parameters c_D , c_E differ from values proposed for light nuclei)

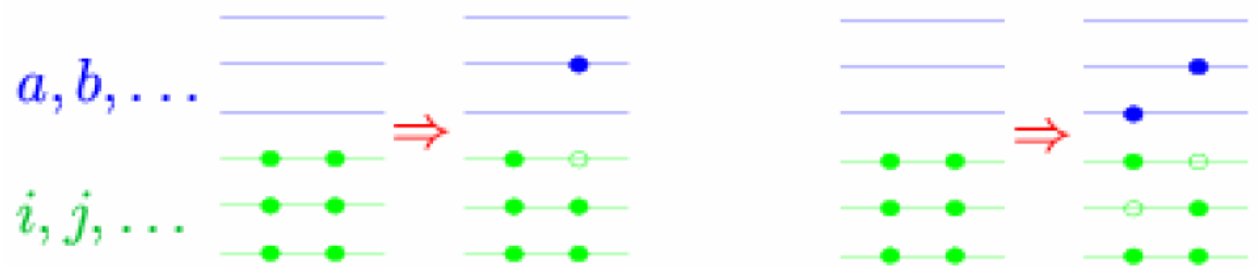
Coupled-cluster method (in CCSD approximation)

Ansatz:

$$\begin{aligned} |\Psi\rangle &= e^T |\Phi\rangle \\ T &= T_1 + T_2 + \dots \\ T_1 &= \sum_{ia} t_i^a a_a^\dagger a_i \\ T_2 &= \sum_{ijab} t_{ij}^{ab} a_a^\dagger a_b^\dagger a_j a_i \end{aligned}$$

- ☺ Scales gently (polynomial) with increasing problem size $\mathcal{O}^2 u^4$.
- ☺ Truncation is the only approximation.
- ☺ Size extensive (error scales with A)
- ☹ Most efficient for doubly magic nuclei

Correlations are *exponentiated* 1p-1h and 2p-2h excitations. Part of np-nh excitations included!



Coupled cluster equations

$$E = \langle \Phi | \bar{H} | \Phi \rangle$$

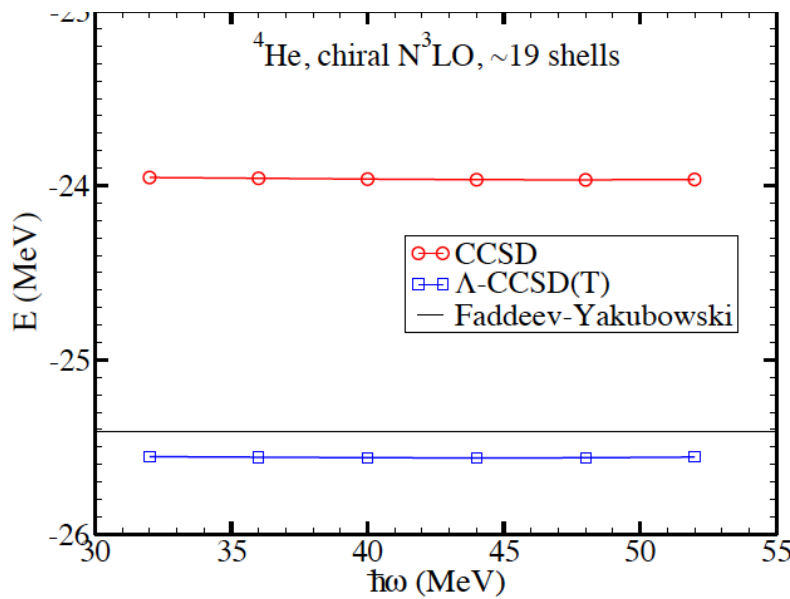
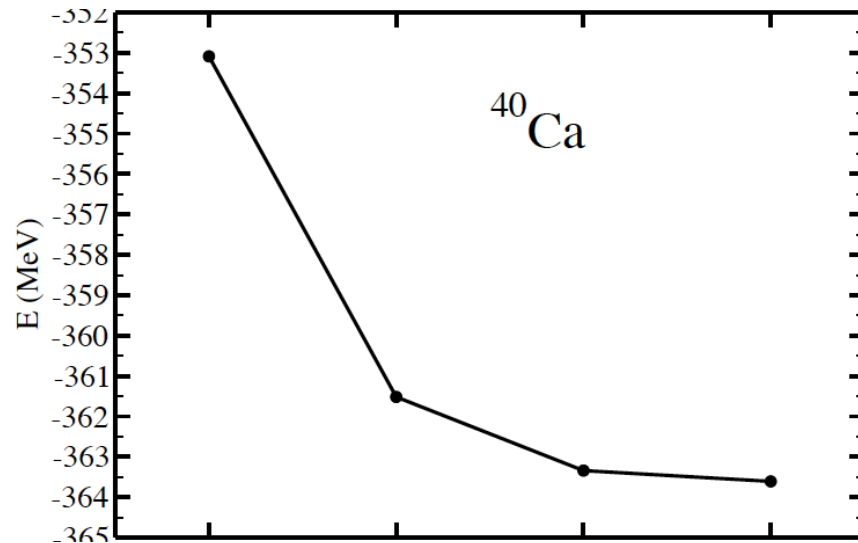
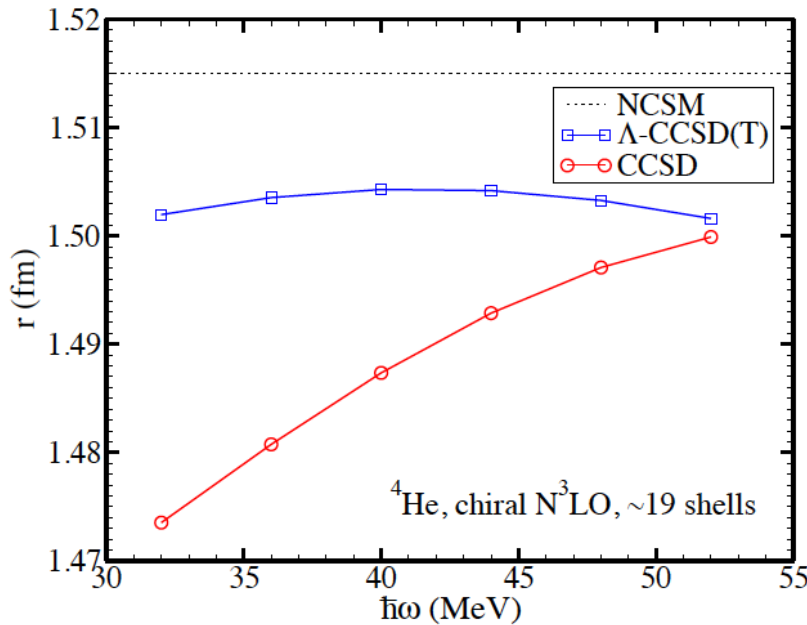
$$0 = \langle \Phi_i^a | \bar{H} | \Phi \rangle$$

$$0 = \langle \Phi_{ij}^{ab} | \bar{H} | \Phi \rangle$$

Alternative view: CCSD generates similarity transformed Hamiltonian with no 1p-1h and no 2p-2h excitations.

$$\bar{H} \equiv e^{-T} H e^T = (H e^T)_c = \left(H + H T_1 + H T_2 + \frac{1}{2} H T_1^2 + \dots \right)_c$$

Benchmarking different methods Chiral N³LO (500 MeV) by Entem & Machleidt, NN only

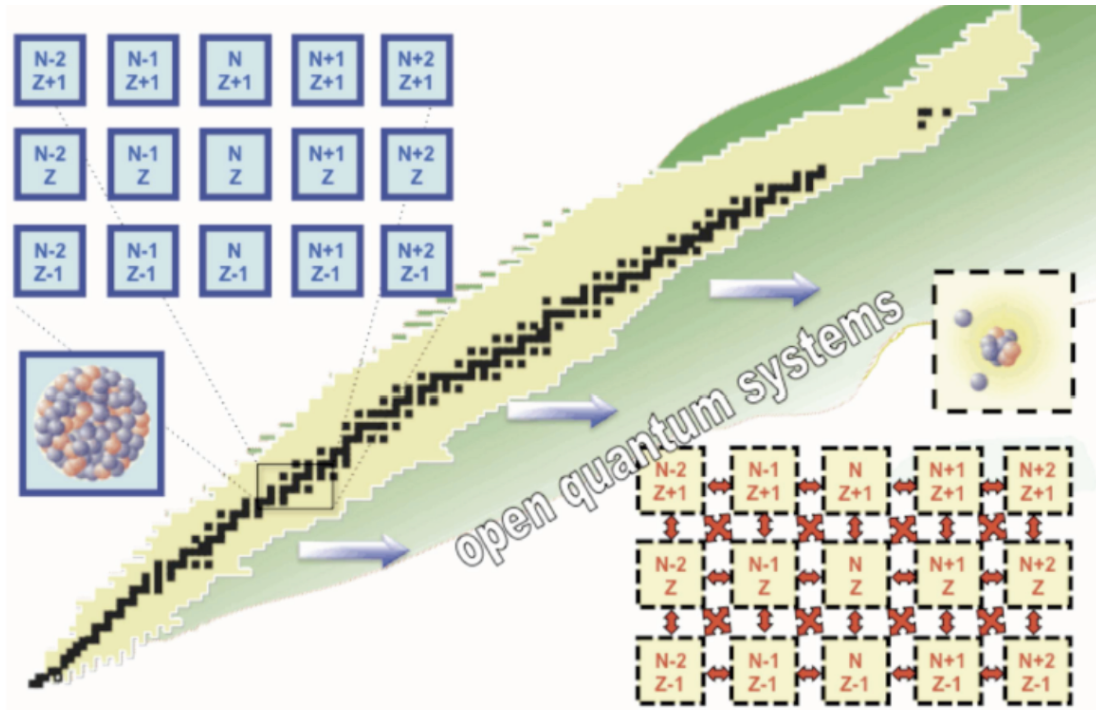


Benchmarking different methods:

Our CC results for ${}^{16}\text{O}$ agree with IT-NCSM (R. Roth et al PRL 107, 072501 (2011)) and UMOA (Fujii et al., Phys. Rev. Lett. 103, 182501 (2009))

	CCM	(IT)-NCSM	UMOA
	E/A	E/A	E/A
${}^4\text{He}$	-6.39(5)	-6.35	
${}^{16}\text{O}$	-7.56(8)	-7.48(4)	-7.47

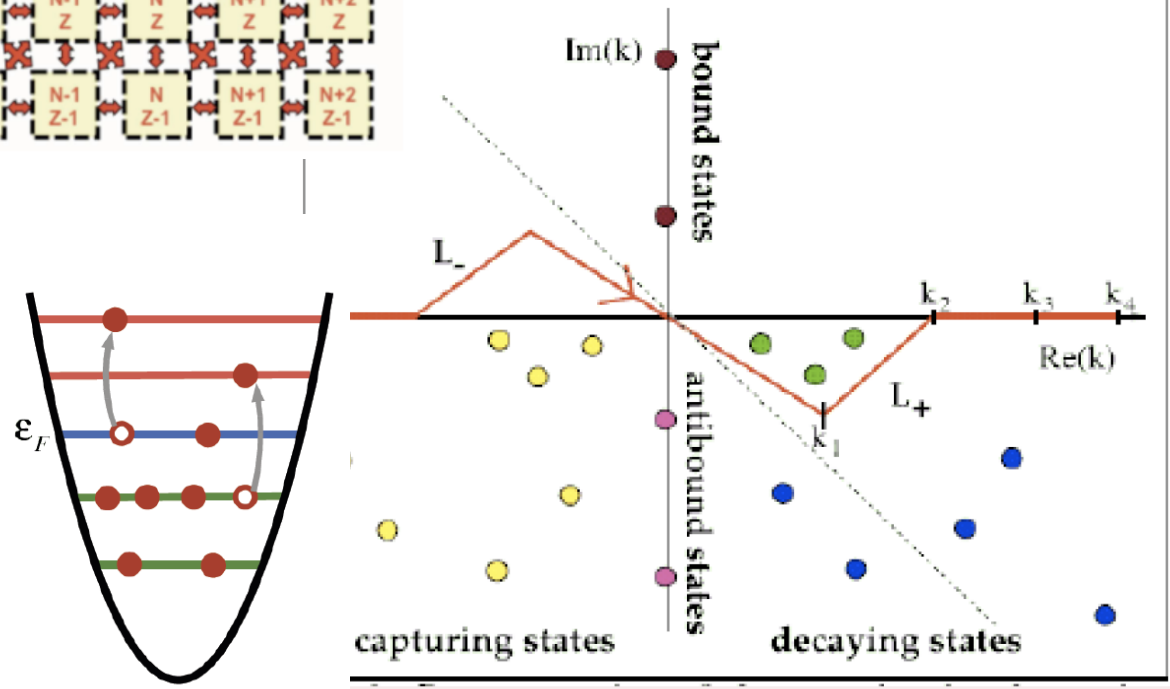
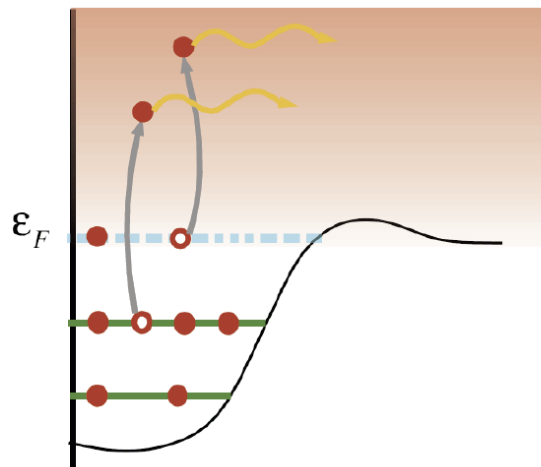
Open Quantum Systems



The Berggren completeness treats bound, resonant and scattering states on equal footing.

Has been successfully applied in the shell model in the complex energy plane to light nuclei. For a review see

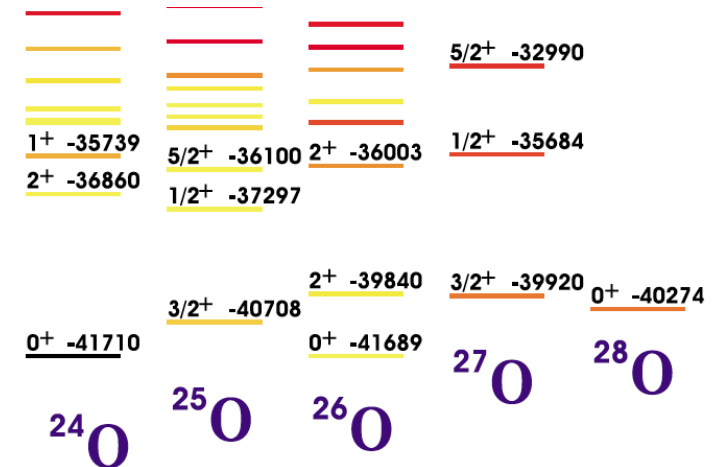
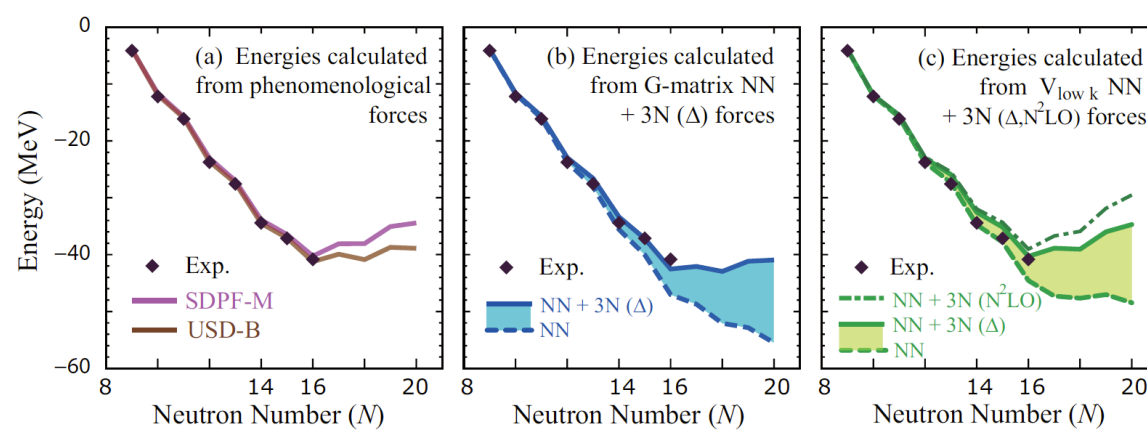
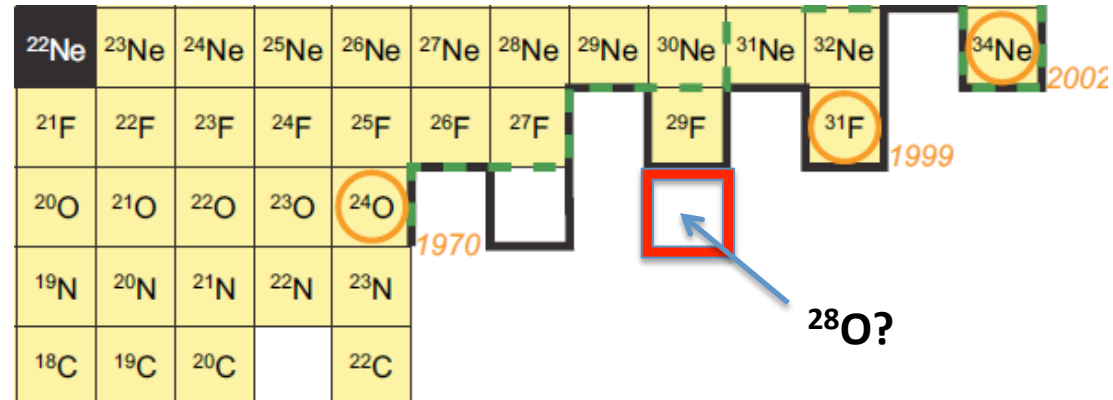
N. Michel et al J. Phys. G 36, 013101 (2009).



Is ^{28}O a bound nucleus?

Experimental situation

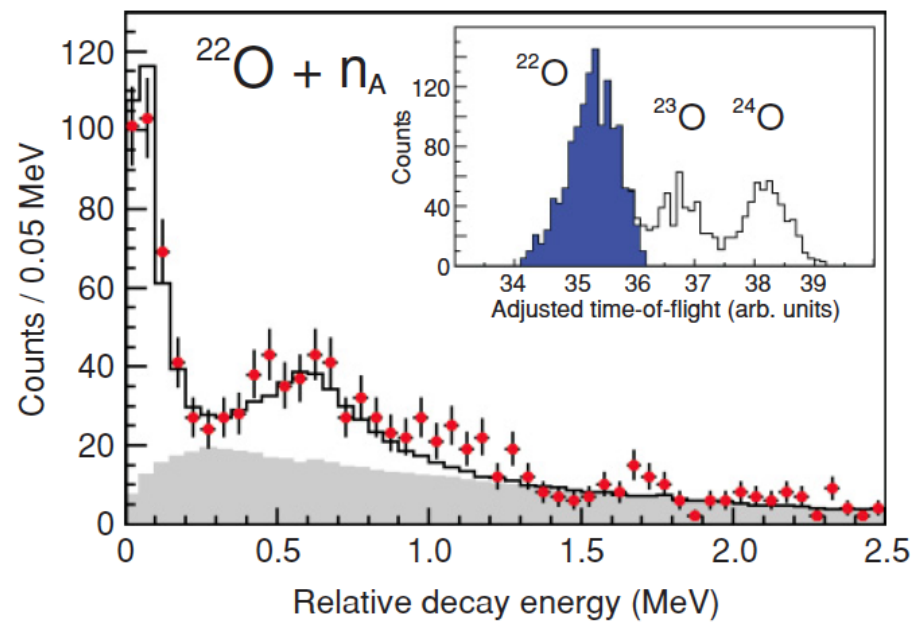
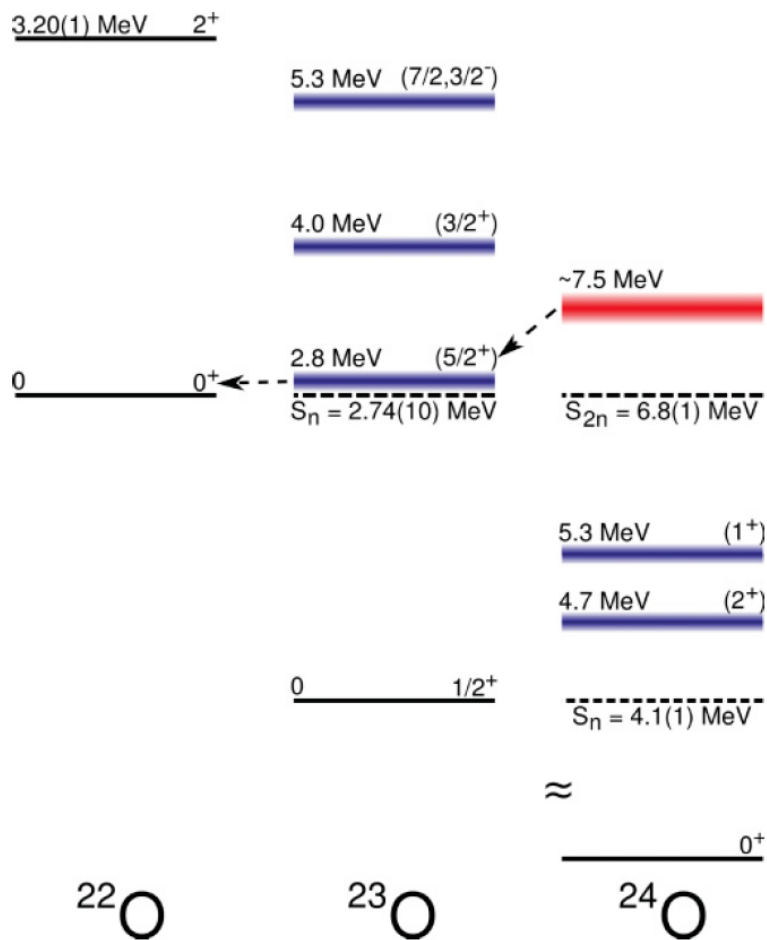
- “Last” stable oxygen isotope ^{24}O
- $^{25,26}\text{O}$ unstable (Hoffman et al 2008, Lunderberg et al 2012)
- ^{28}O not seen in experiments
- ^{31}F exists (adding on proton shifts drip line by 6 neutrons!?)



Continuum shell model with HBUSD interaction predict ^{28}O unbound. A. Volya and V. Zelevinsky PRL (2005)

Shell model (sd shell) with monopole corrections based on three-nucleon force predicts ^{24}O as last stable isotope of oxygen. [Otsuka, Suzuki, Holt, Schwenk, Akaishi, PRL (2010), arXiv:0908.2607]

Resonances in neutron rich oxygen-24



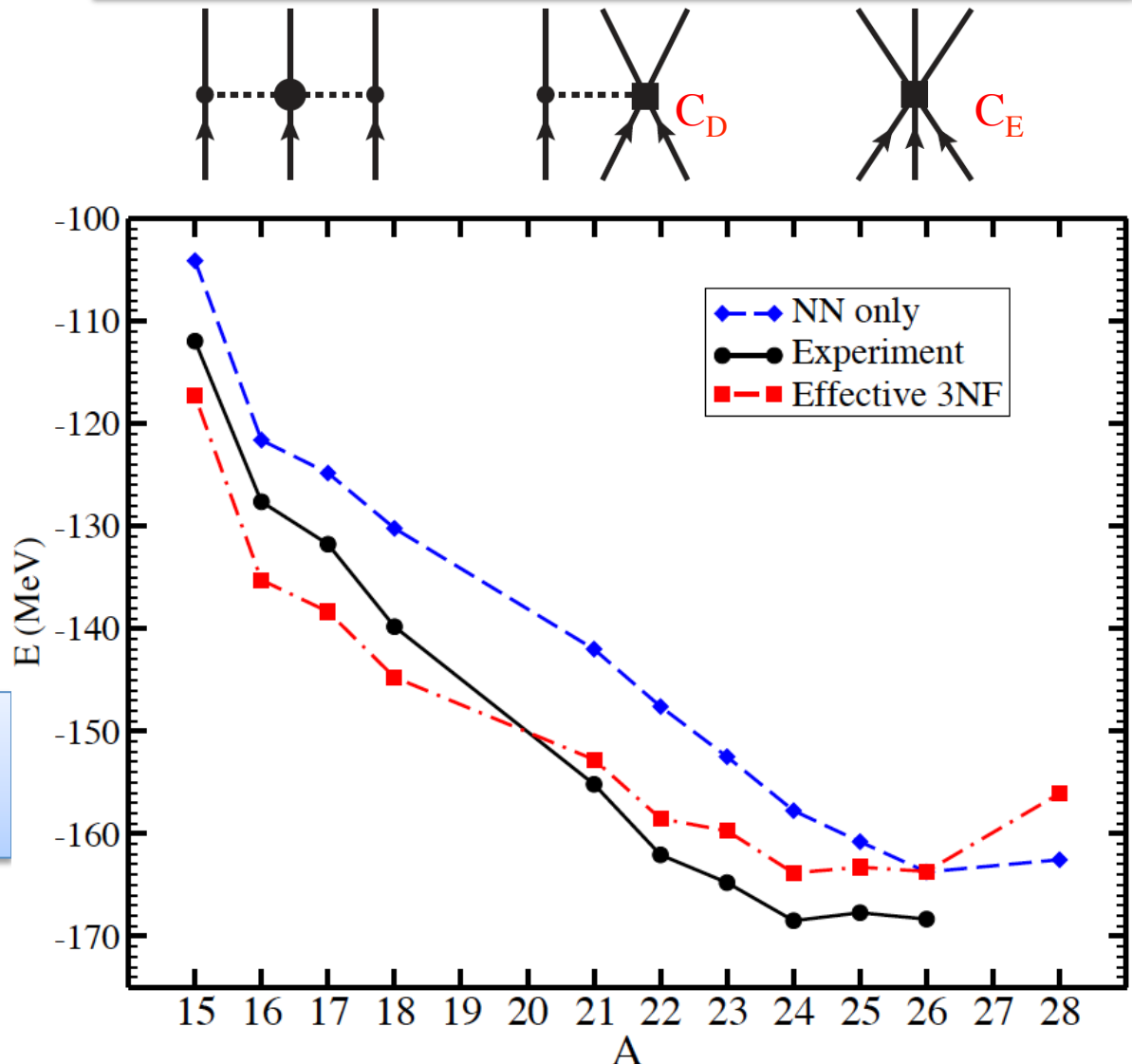
C. R. Hoffman et al Phys. Rev. C **83**, 031303(R) (2011)

- Knockout reaction of ^{26}F reveal a resonance above the two-neutron threshold in ^{24}O
- No spin and parity assigned of this state
- A challenge for microscopic theory to address these states

Oxygen isotopes from chiral interactions

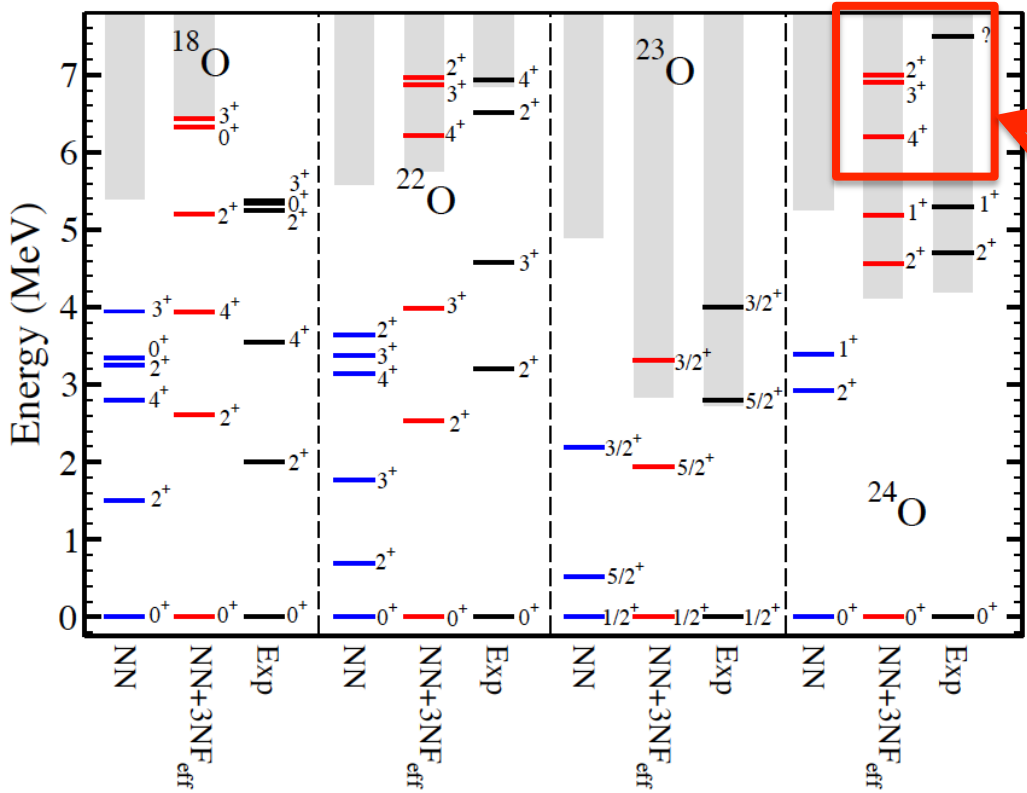
- Inclusion of effective 3NF places dripline at ^{25}O .
- Overall the odd-even staggering in the neutron rich oxygen is well reproduced.
- We find ^{26}O to be unbound with respect to ^{24}O by $\sim 100\text{keV}$, agreement with E. Lunderberg et al., Phys. Rev. Lett. 108 (2012) 142503
- We find ^{28}O to be unbound with a resonance width of $\sim 2\text{MeV}$

Chiral three-nucleon force at order N2LO. $k_f = 1.05\text{fm}^{-1}$, $C_D = 0.2$, $C_E = 0.71$ (fitted to the binding energy of ^{16}O and ^{22}O).



G. Hagen, M. Hjorth-Jensen, G. R. Jansen, R. Machleidt, T. Papenbrock, Phys. Rev. Lett. 108, 242501 (2012).

Oxygen isotopes from chiral interactions

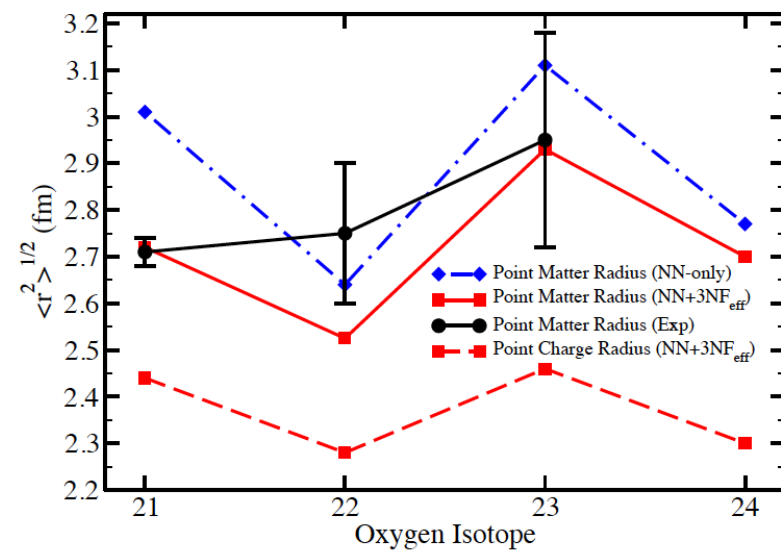


The effects of three-nucleon forces decompress the spectra and brings it in good agreement with experiment.

We find several states ($4^+, 3^+, 2^+$) near the observed peak at $\sim 7.5\text{MeV}$ in ^{24}O

C. R. Hoffman et al Phys. Rev. C **83**, 031303 (2011)

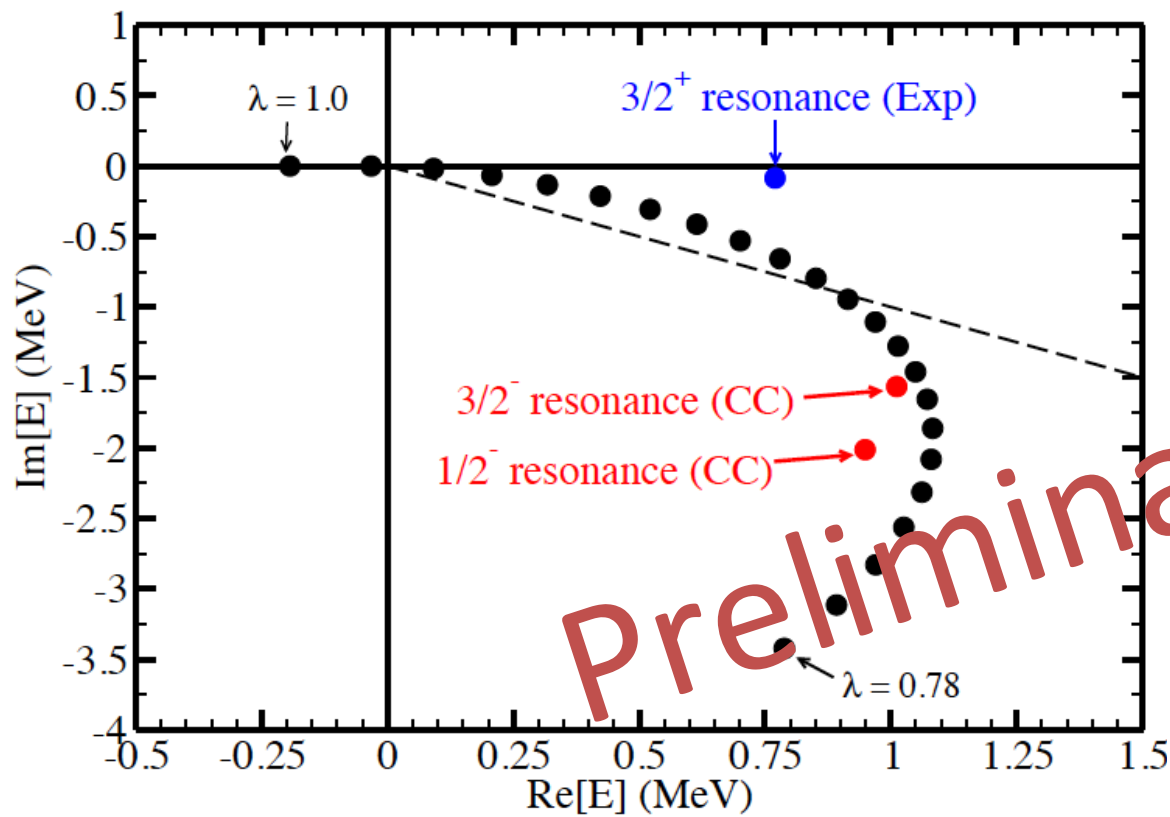
Matter and charge radii for $^{21-24}\text{O}$
Computed from intrinsic densities and
Compared to experiment.



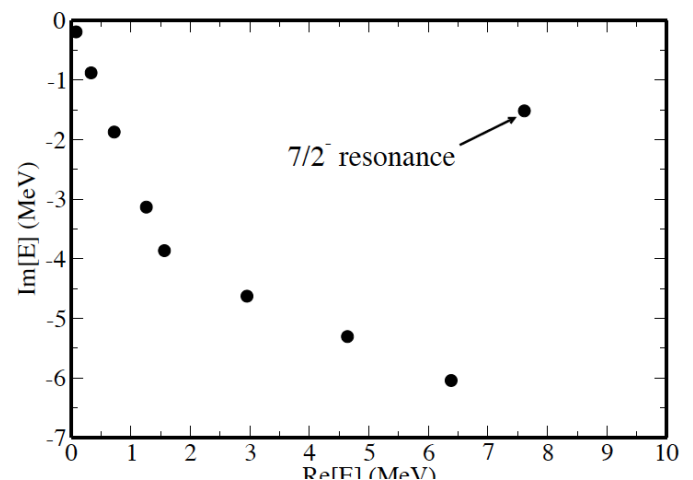
Excited states in ^{24}O computed with EOM-CCSD and compared to experiment

J^π	2^+_1	1^+_1	4^+_1	3^+_1	2^+_2	1^+_2
E_{CC}	4.56	5.2	6.2	6.9	7.0	8.4
E_{Exp}	4.7(1)	5.33(10)				
Γ_{CC}	0.03	0.04	0.005	0.01	0.04	0.56
Γ_{Exp}	$0.05^{+0.21}_{-0.05}$	$0.03^{+0.12}_{-0.03}$				

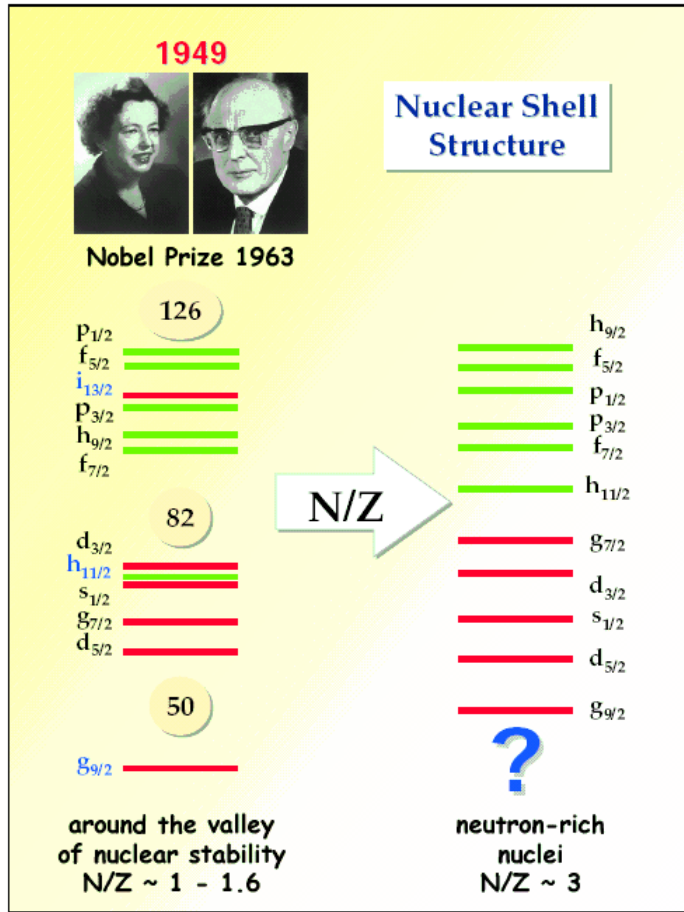
Negative parity states in ^{25}O ?



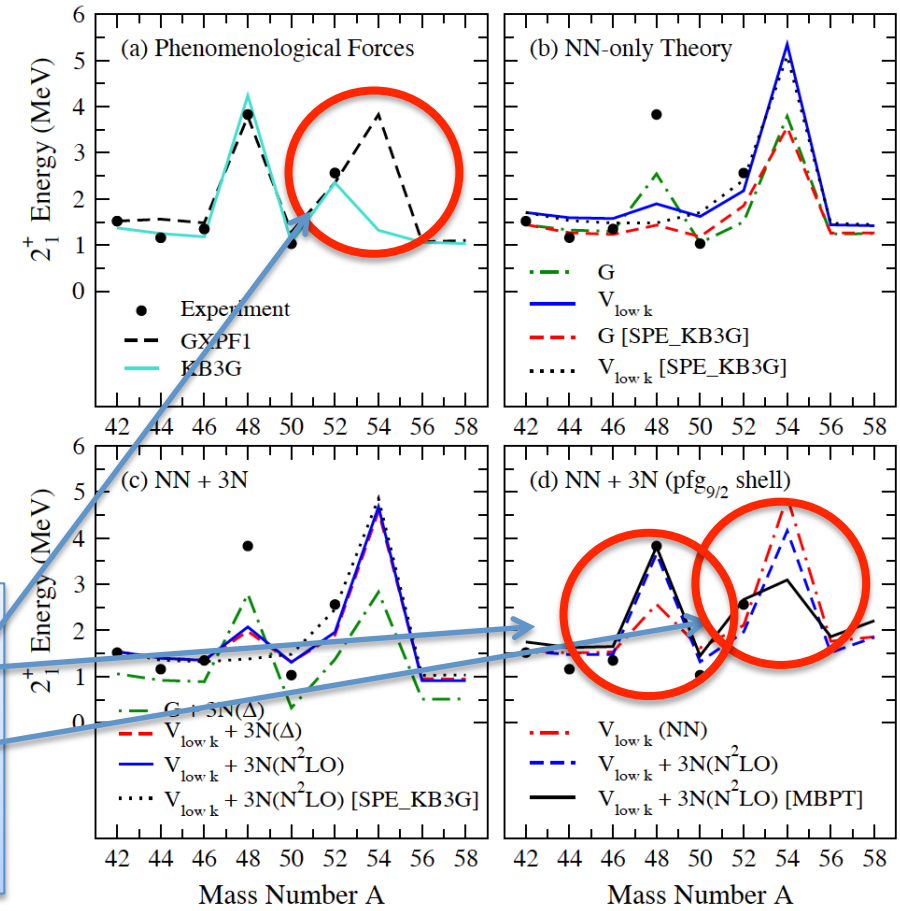
- Low-lying $3/2^-$ and $1/2^-$ intruder states close to the $3/2^+$ groundstate in ^{25}O
- Due to very large width of these states they will be difficult to measure.
- Simple Woods-Saxon model agrees with CC results.



Evolution of shell structure in neutron rich Calcium



- How do shell closures and magic numbers evolve towards the dripline?
- Is the naïve shell model picture valid at the neutron dripline?



- 3NFs are responsible for shell closure in ^{48}Ca
- Different models give conflicting result for shell closure in ^{54}Ca .

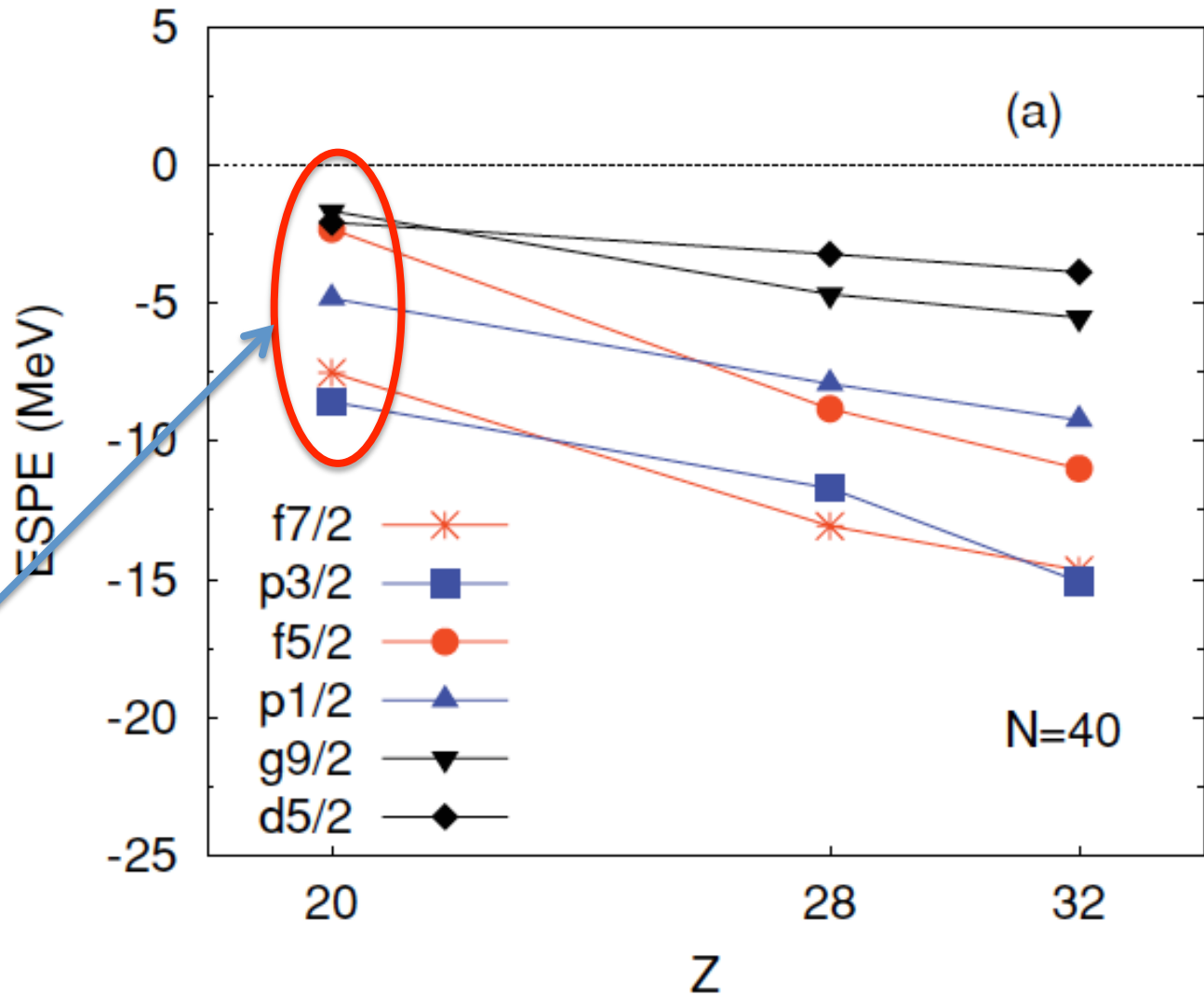
J. D. Holt et al, J. Phys. G 39, 085111 (2012)

Evolution of shell structure in neutron rich Calcium

Inversion of shell order in ^{60}Ca

S. M. Lenzi, F. Nowacki, A. Poves, and K. Sieja Phys. Rev. C 82, 054301 (2010)

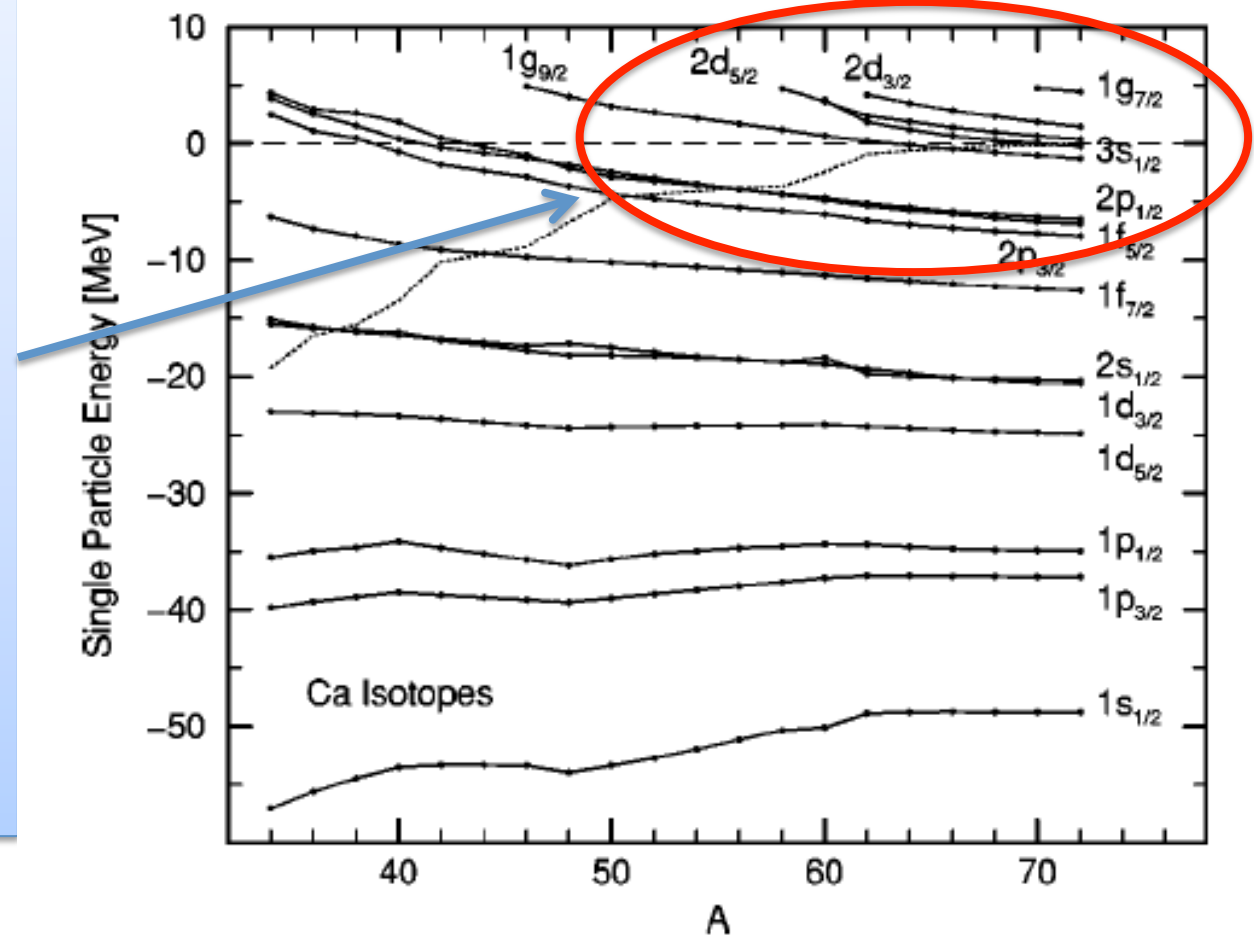
- Inversion of $d5/2$ and $g9/2$ in ^{60}Ca .
- Bunching of levels pointing to no shell-closure.



Evolution of shell structure in neutron rich Calcium

- Relativistic mean-field show no shell gap in $^{60-70}\text{Ca}$
- Bunching of single-particle orbitals
- large deformations and no shell closure

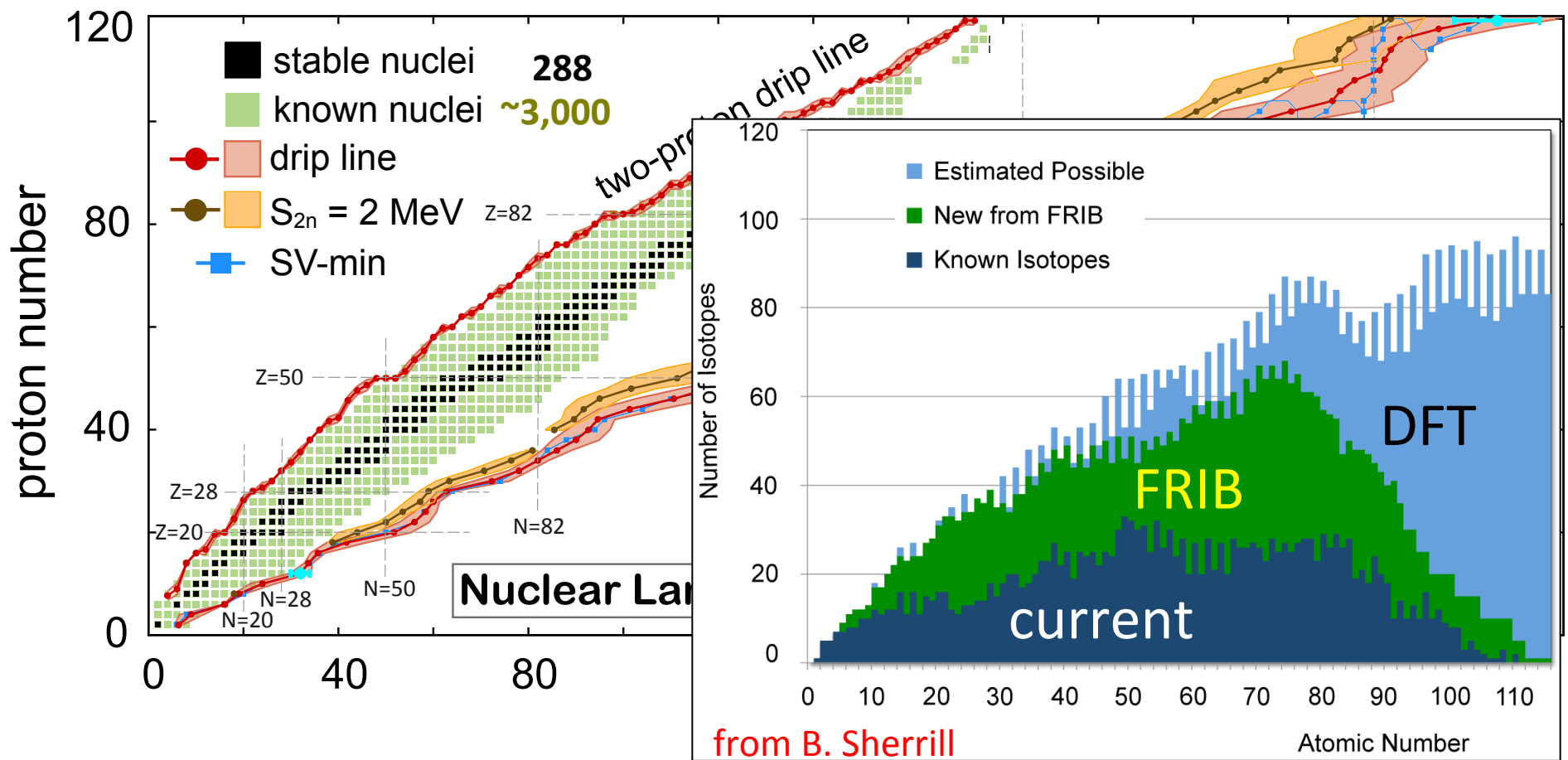
J. Meng et al, Phys. Rev. C 65, 041302(R) (2002)



How many protons and neutrons can be bound in a nucleus?

Literature: 5,000-12,000

Skyrme-DFT: $6,900 \pm 500_{\text{syst}}$

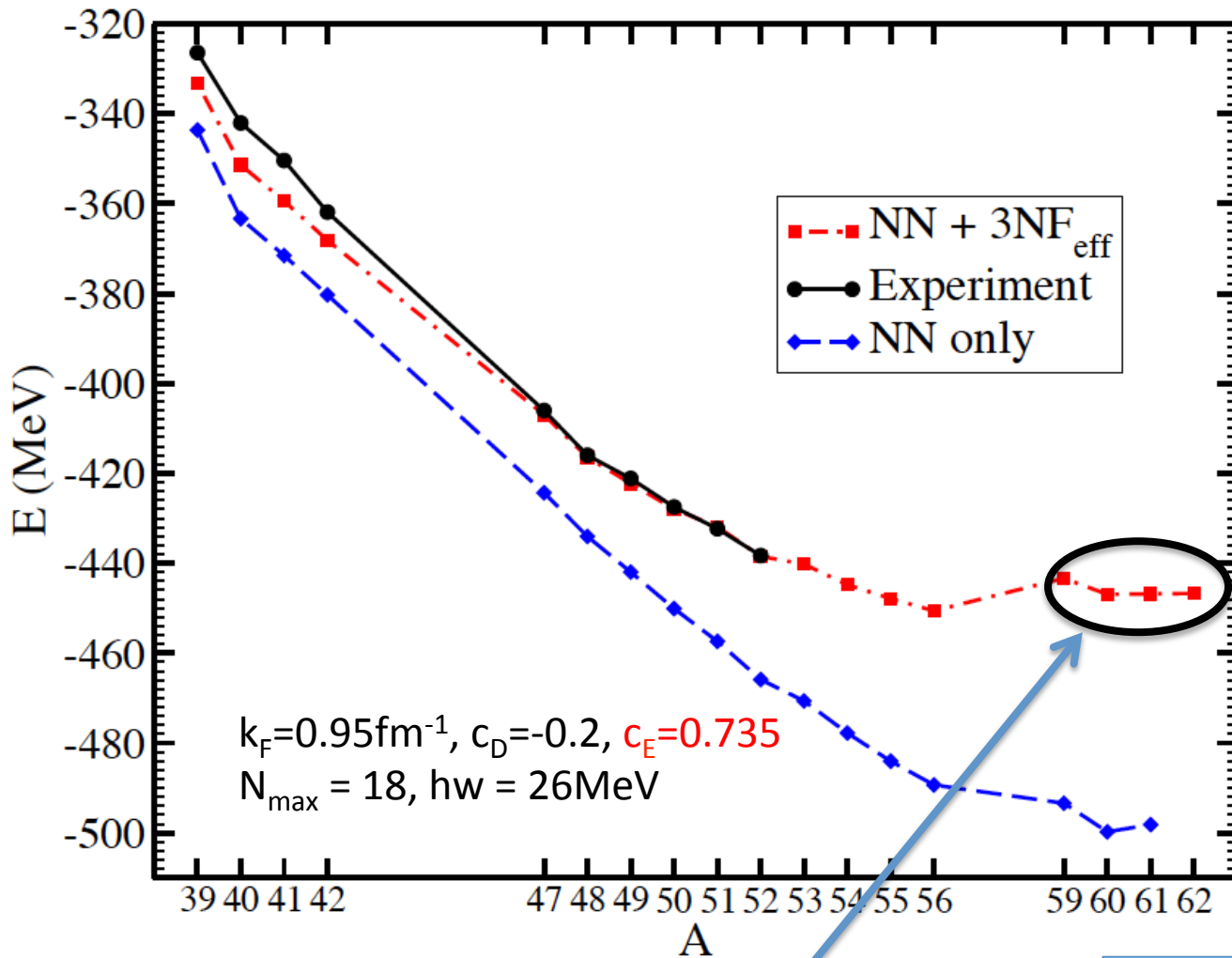


Description of observables and model-based extrapolation

- Systematic errors (due to incorrect assumptions/poor modeling)
- Statistical errors (optimization and numerical errors)

Erler et al., Nature 486, 509 (2012)

Calcium isotopes from chiral interactions

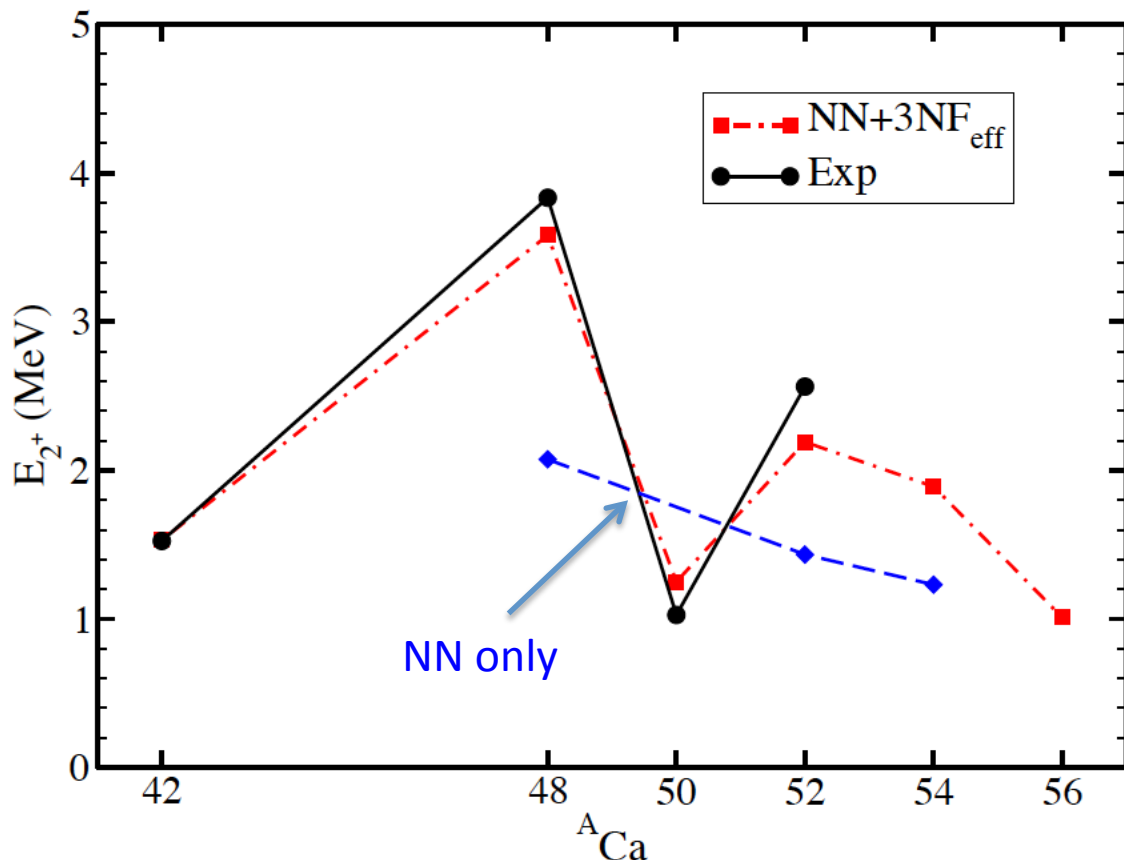


Main Features:

1. Total binding energies agree well with experimental masses.
2. Masses for $^{40-52}\text{Ca}$ are converged in 19 major shells.
3. ^{60}Ca is not magic
4. $^{61-62}\text{Ca}$ are located right at threshold.

G. Hagen, M. Hjorth-Jensen, G. R. Jansen, R. Machleidt, T. Papenbrock, Phys. Rev. Lett. 109, 032502 (2012).

2^+ systematics in Calcium isotopes



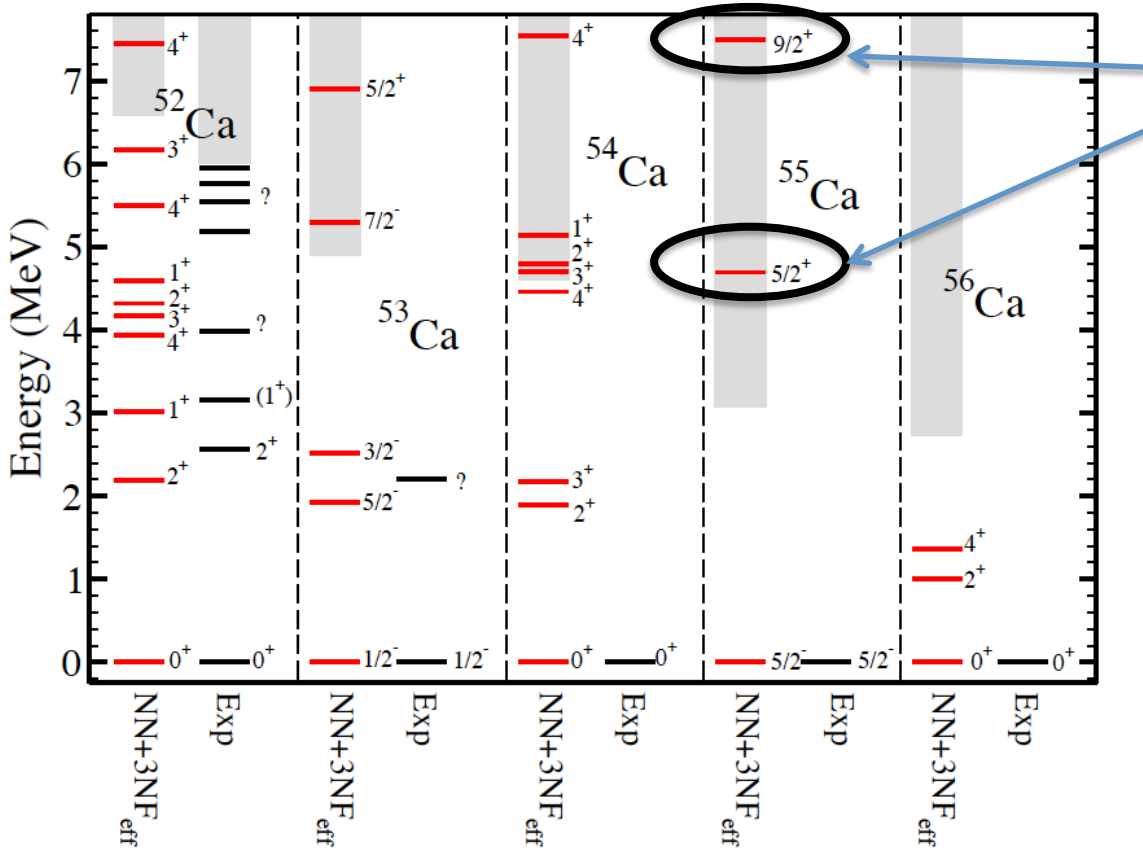
Main Features:

1. Good agreement between theory and experiment.
2. Shell closure in ^{48}Ca due to effects of 3NFs
3. Predict weak (sub-)shell closure in ^{54}Ca .

G. Hagen, M. Hjorth-Jensen, G. R. Jansen, R. Machleidt, T. Papenbrock, Phys. Rev. Lett. 109, 032502 (2012).

	^{48}Ca			^{52}Ca			^{54}Ca		
	2^+	4^+	$4^+/2^+$	2^+	4^+	$4^+/2^+$	2^+	4^+	$4^+/2^+$
CC	3.58	4.20	1.17	2.19	3.95	1.80	1.89	4.46	2.36
Exp	3.83	4.50	1.17	2.56	?	?	?	?	?

Spectra and shell evolution in Calcium isotopes



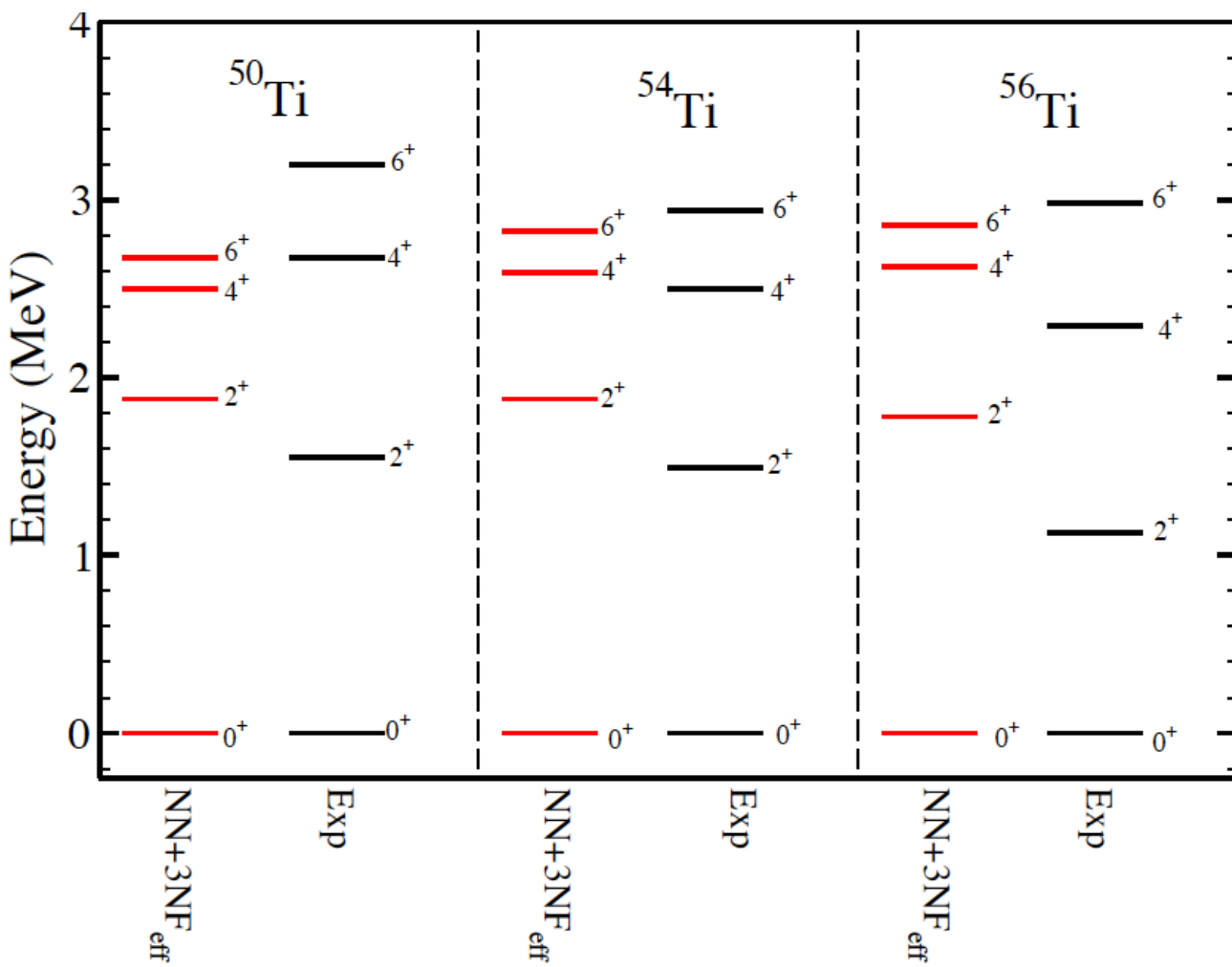
1. Inversion of the 9/2+ and 5/2+ resonant states in $^{53,55,61}\text{Ca}$
2. We find the ground state of ^{61}Ca to be $\frac{1}{2}+$ located right at threshold.
3. A harmonic oscillator basis gives the naïve shell model ordering of states.
4. Continuum coupling is crucial.

	^{48}Ca	^{52}Ca	^{54}Ca
E_{2+} (CC)	3.58	2.19	1.89
E_{2+} (Exp)	3.83	2.56	n.a.
E_{4+}/E_{2+} (CC)	1.17	1.80	2.36
E_{4+}/E_{2+} (Exp)	1.17	n.a.	n.a.
S_n (CC)	9.45	6.59	4.59
S_n (Exp)	9.95	6.0*	4.0†

New penning trap measurement of masses of $^{51,52}\text{Ca}$
A. T. Gallant et al Phys. Rev. Lett. **109**, 032506 (2012)

J^π	^{53}Ca		^{55}Ca		^{61}Ca	
	Re[E]	Γ	Re[E]	Γ	Re[E]	Γ
$5/2^+$	1.99	1.97	1.63	1.33	1.14	0.62
$9/2^+$	4.75	0.28	4.43	0.23	2.19	0.02

Check of method and interaction: Titanium isotopes



Main Features:

1. Two-particle attached coupled-cluster approach to Titanium isotopes.
2. Good agreement with experiment.
3. 2p-0h amplitudes account for about 60% of the total amplitude for the isotopes of titanium, while this number is about 72% for the calcium isotopes

Towards nuclear reactions with coupled-cluster theory

One-nucleon overlap functions

Elastic scattering, capture and transfer reactions of a nucleon on/to a target nucleus with mass A is determined by the one-nucleon overlap function

$$O_A^{A+1}(lj; r) = \langle A \parallel \tilde{a}_{lj}(r) \parallel A + 1 \rangle = \sum_n \langle A \parallel \tilde{a}_{nlj} \parallel A + 1 \rangle \phi_{nlj}(r)$$

Microscopic definition of Spectroscopic Factors

SF is the norm of the overlap function and quantifies the degree of correlations
SFs are not observables and depend on the resolution scale

$$SF = \int_0^\infty dr r^2 |O_A^{A+1}(lj; r)|^2$$

Asymptotic properties of the one-nucleon overlap functions

The overlap functions satisfy a one-body Schrodinger like equation, and outside the range of the interaction the overlap function is proportional to a single-particle wave function

$$O_A^{A+1}(lj; r) = C \frac{e^{-\kappa r}}{\kappa r}$$

Bound states

$$O_A^{A+1}(lj; r) = A (j_l(kr) - \tan \delta_l n_l(kr))$$

Scattering states

Treatment of long-range Coulomb effects

We write the Coulomb interaction

$$V_{\text{Coul}} = U_{\text{Coul}}(r) + [V_{\text{Coul}} - U_{\text{Coul}}(r)]$$

Demanding

$$U_{\text{Coul}}(r) \rightarrow (Z-1)e^2/r \text{ for } r \rightarrow +\infty$$

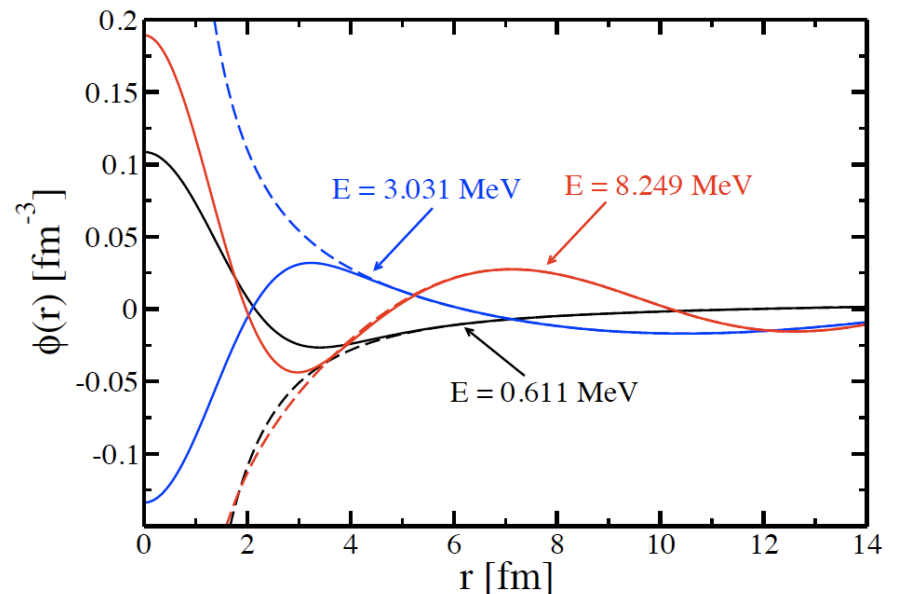
The second term is short range and can be expanded in Harmonic Oscillator basis. The first term contain the long range Coulomb part:

$$\begin{aligned} U_{\text{Coul}}(k, k') = & \langle k | U_{\text{Coul}}(r) - \frac{(Z-1)e^2}{r} | k' \rangle + \\ & \frac{(Z-1)e^2}{\pi} Q_\ell \left(\frac{k^2 + k'^2}{2kk'} \right) \end{aligned}$$

We diagonalize the one-body Schrödinger equation in momentum space using the off-diagonal method

N. Michel Phys. Rev. C 83, 034325 (2011)

N_R	N_T	$s_{1/2}$		$d_{3/2}$		$d_{5/2}$	
		Re[E]	Γ	Re[E]	Γ	Re[E]	Γ
5	15	1.1054	0.1446	5.0832	1.3519	1.4923	0.0038
5	20	1.1033	0.1483	5.0785	1.3525	1.4873	0.0079
10	25	1.0989	0.1360	5.0765	1.3525	1.4858	0.0093
10	30	1.0986	0.1366	5.0757	1.3529	1.4849	0.0103
15	40	1.0978	0.1351	5.0749	1.3531	1.4842	0.0111
15	50	1.0978	0.1353	5.0746	1.3533	1.4838	0.0114
20	60	1.0976	0.1349	5.0745	1.3533	1.4837	0.0116
30	70	1.0975	0.1346	5.0744	1.3534	1.4837	0.0117
(Michel 2011)		1.0975	0.1346	5.0744	1.3535	1.4836	0.0119



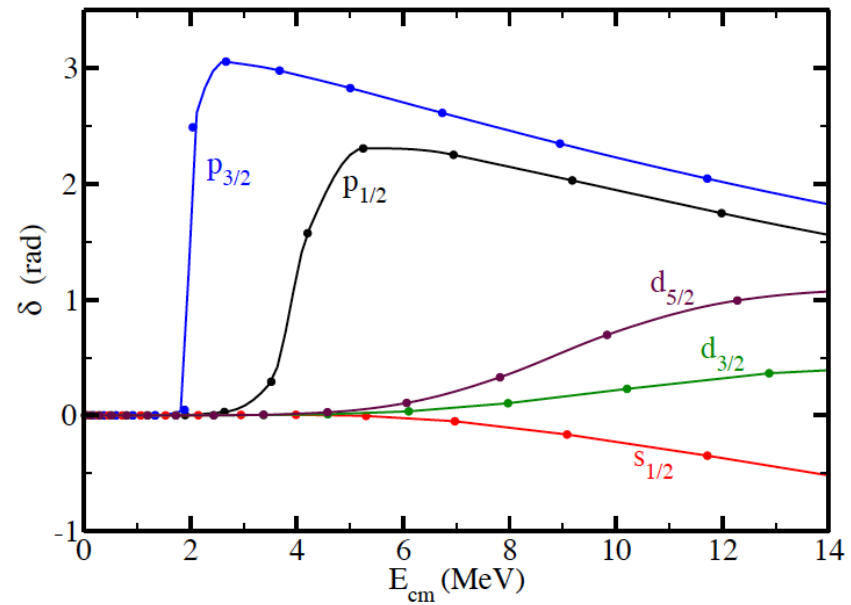
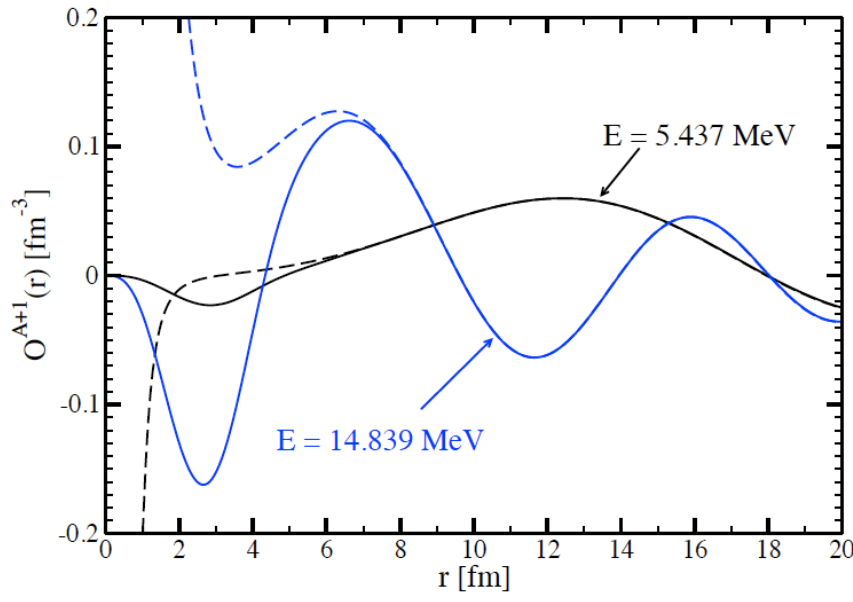
Elastic proton/neutron scattering on ^{40}Ca

The one-nucleon overlap function: $O_A^{A+1}(lj; kr) = \oint_n \left\langle A + 1 \middle\| \tilde{a}_{nlj}^\dagger \middle\| A \right\rangle \phi_{nlj}(r).$

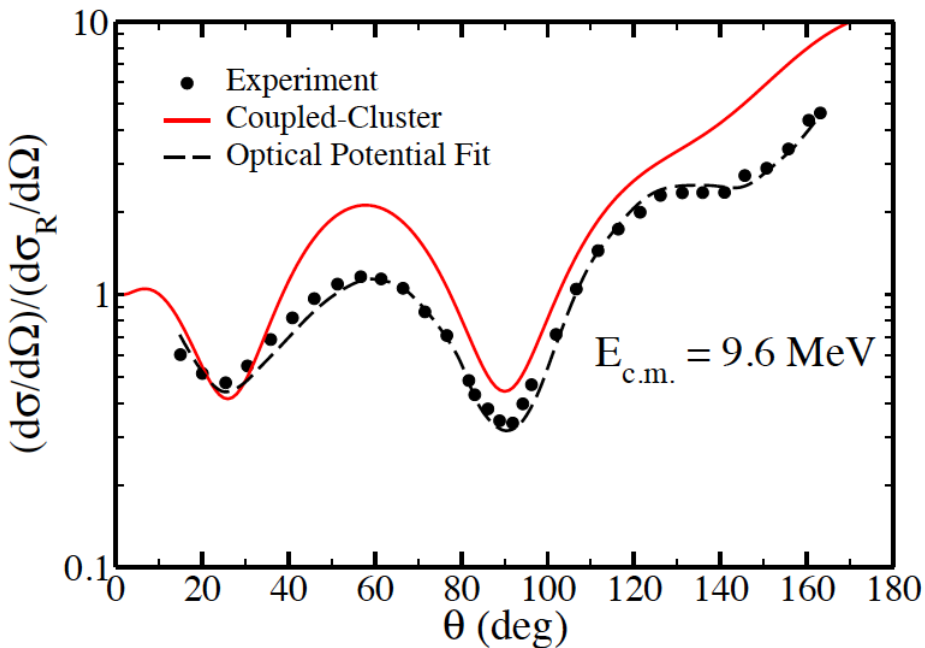
Beyond the range of the nuclear interaction the overlap functions take the form:

$$O_A^{A+1}(lj; kr) = C_{lj} \frac{W_{-\eta, l+1/2}(kr)}{r}, \quad k = i\kappa$$

$$O_A^{A+1}(lj; kr) = C_{lj} [F_{\ell, \eta}(kr) - \tan \delta_l(k) G_{\ell, \eta}(kr)]$$



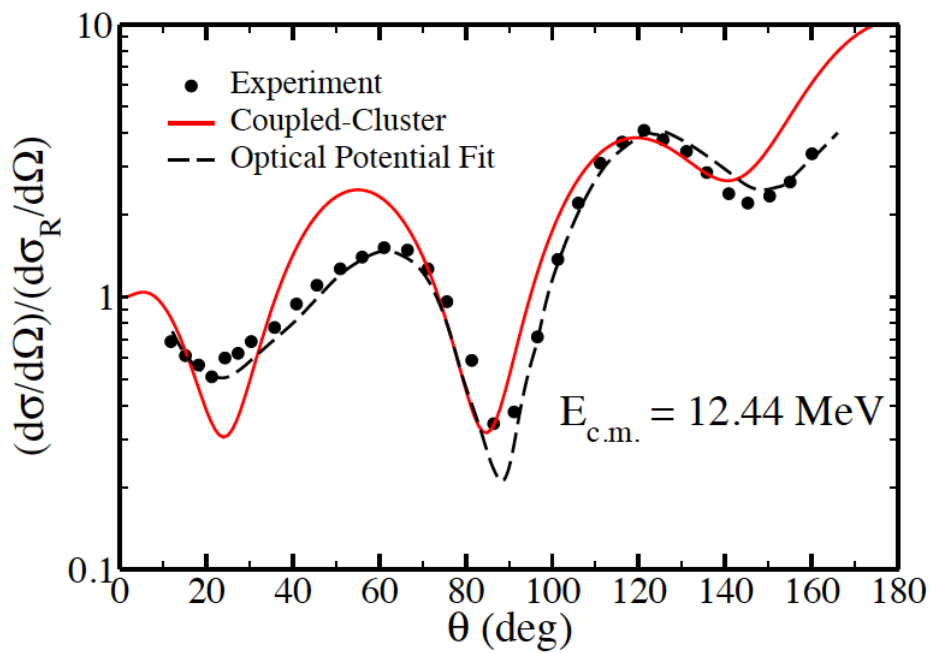
Elastic proton/neutron scattering on ^{40}Ca



Differential cross section for elastic proton scattering on ^{40}Ca .

Fair agreement between theory and experiment for low-energy scattering.

G. Hagen and N. Michel
Phys. Rev. C 86, 021602(R) (2012).



Densities and radii from coupled-cluster theory

We solve for the right and left ground state of the similarity transformed Hamiltonian

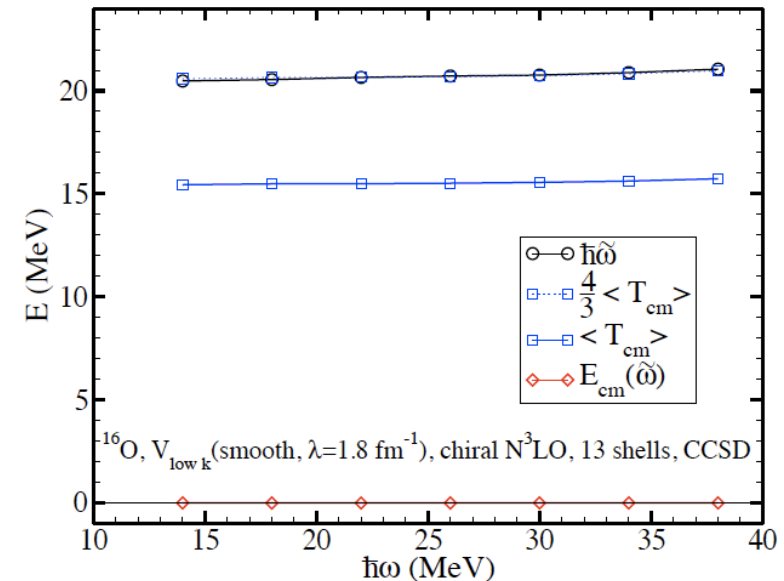
$$e^{-T} H_N e^T |\phi_0\rangle = \overline{H_N} |\phi_0\rangle = E_{CC} |\phi_0\rangle \quad \langle \phi_0 | L_0 \overline{H_N} = E_{CC} \langle \phi_0 | L_0$$

The density matrix is computed within coupled-cluster method as:

$$\rho_{pq} = \langle \Psi_0 | a_p^\dagger a_q | \Psi_0 \rangle = \langle \phi_0 | L e^{-T} a_p^\dagger a_q e^T | \phi_0 \rangle = \langle \phi_0 | L a_p^\dagger a_q | \phi_0 \rangle$$

The coupled-cluster wave function factorizes to a good approximation into an intrinsic and center of mass part, $\Psi = \psi_{in} \Gamma$ where the center of mass part is a Gaussian with a fixed oscillator frequency independent of single-particle basis

GH, T. Papenbrock and D. Dean et al, Phys. Rev. Lett. **103**, 062503 (2009)



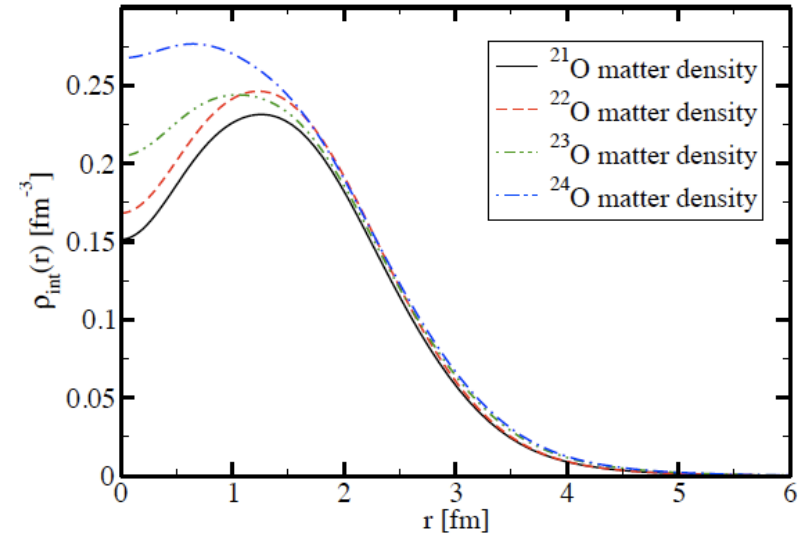
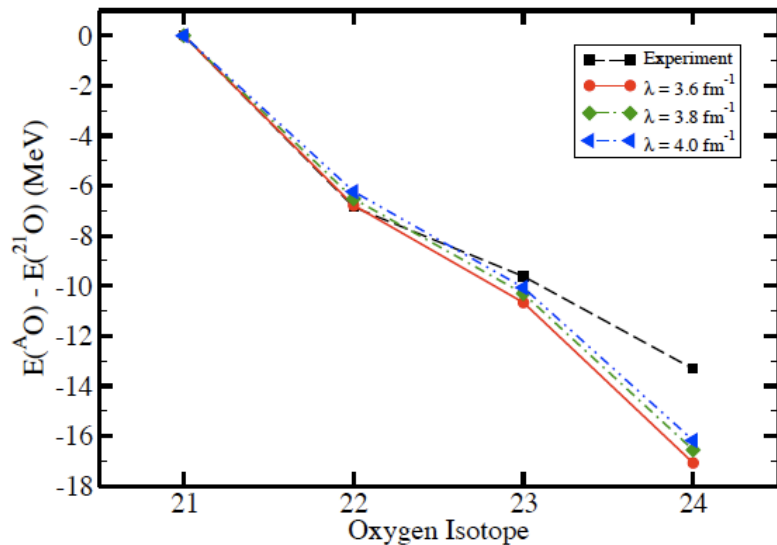
We can obtain the intrinsic density by a deconvolution of the laboratory density

B. G. Giraud, Phys. Rev. C **77**, 014311 (2008)

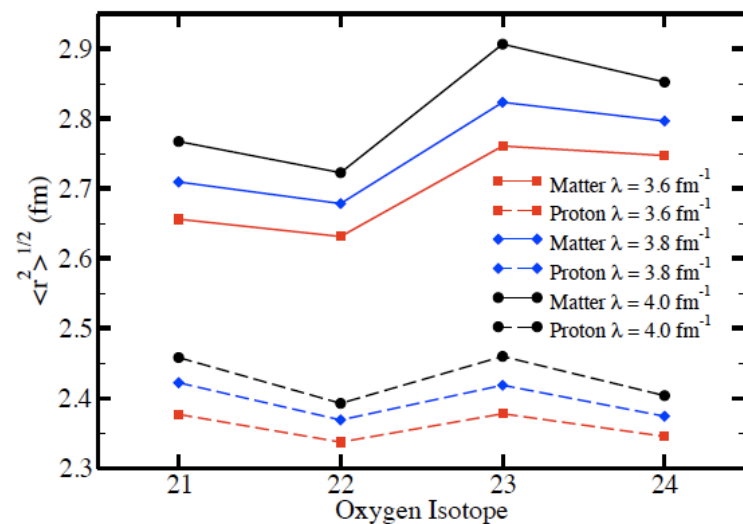
$$A^{-1} \rho(r) = A^{-1} \int dR [\Gamma(R)]^2 \sigma \left[\frac{A}{A-1} (r-R) \right]$$

↑ Lab. density
 ↑ Center of mass part
 ↑ Intrinsic density

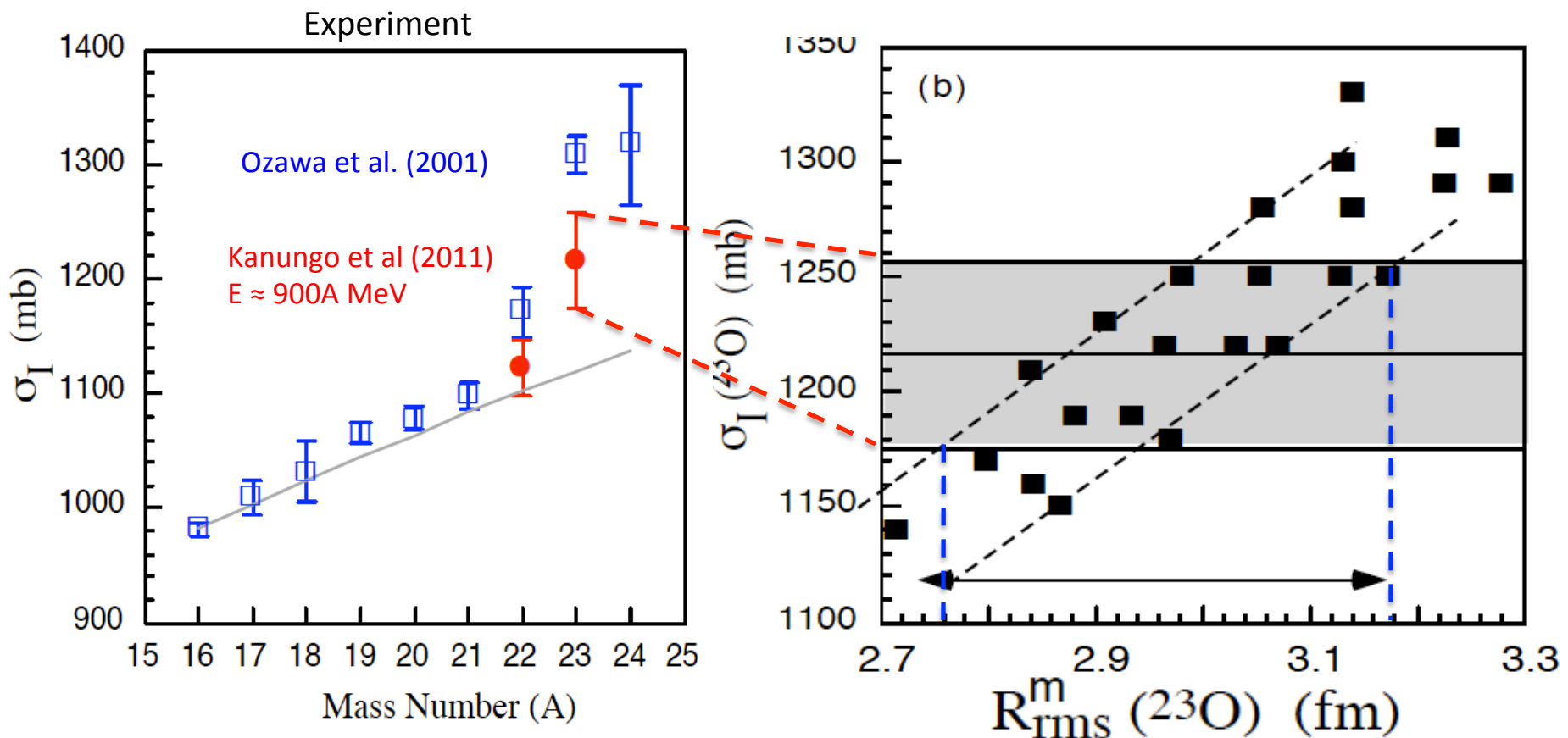
Densities and radii from coupled-cluster theory



1. Relative energies in $^{21-24}\text{O}$ depend weakly on the resolution scale
2. We clearly see shell structure appearing in the matter densities for $^{21-24}\text{O}$
3. Matter and charge radii depend on the resolution scale, however relative difference which is relevant for isotope shift measurements does not



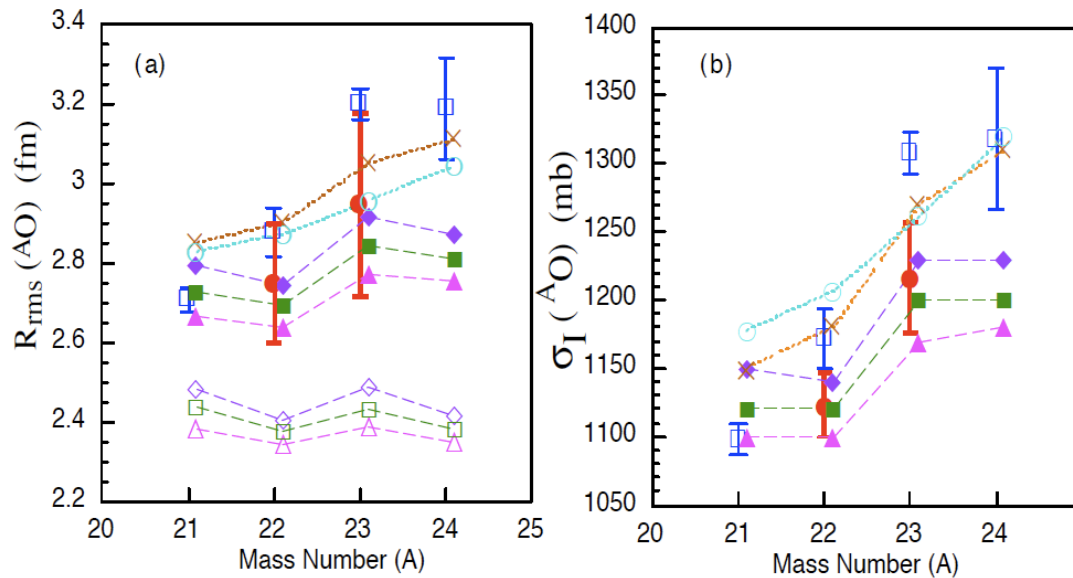
^{23}O interaction cross section (scattering off ^{12}C target @ GSI)



Experimental radii extracted from matter distribution within Glauber model.
Main result of new measurement: ^{23}O follows systematics; interaction cross section consistent with separation energies.

R. Kanungo *et al* Phys. Rev. C **84**, 061304 (2011)

Resolving the anomaly in the cross section of ^{23}O



The anomaly of ^{23}O

New measurements (R. Kanungo) of the ^{23}O cross section and coupled cluster calculations show that ^{23}O is not consistent with a one-neutron halo picture

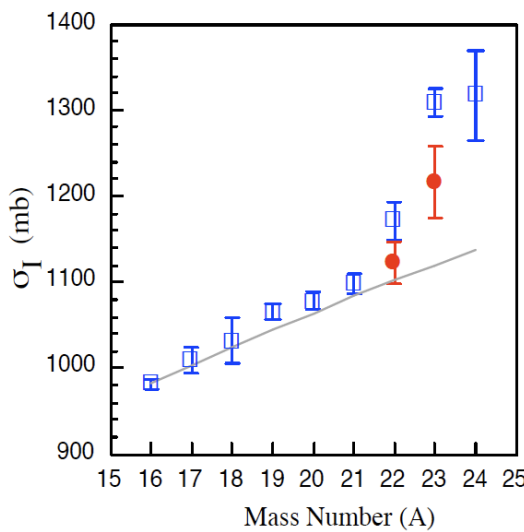


TABLE I: Measured interaction cross sections and the root mean square point matter radii (R_{rms}^m (ex.)) for $^{22-23}\text{O}$.

Isotope	$\sigma_I(\Delta\sigma)$ (mb)	$\Delta\sigma(\text{Stat.})$ (mb)	$\Delta\sigma(\text{Syst.})$ (mb)	R_{rms}^m (ex.) (fm)
^{22}O	1123(24)	18.5	15.3	2.75 ± 0.15
^{23}O	1216(41)	33.1	24.7	2.95 ± 0.23

Summary

1. Interactions from Chiral EFT probed in nuclei
2. CC calculations for oxygen and calcium with effects of 3NF and continuum give significant improvement in binding energy and spectra.
3. Predict spin and parity of newly observed resonance peak in ^{24}O .
4. Predict weak sub-shell closure in ^{54}Ca .
5. Level ordering in the gds shell in neutron calcium is reversed compared to naïve shell model.
6. Elastic proton scattering on medium mass nuclei from coupled-cluster theory
7. Densities from coupled-cluster – Anomalous large cross section in ^{23}O resolved